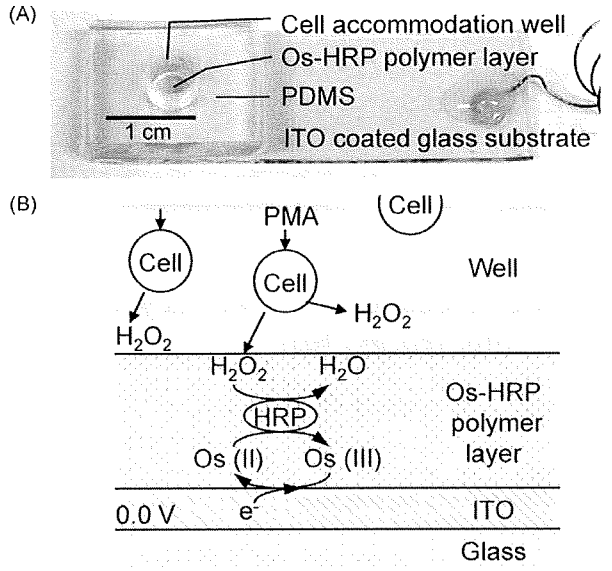

Fig. 1. (A) Photograph of the electrode chip with a PDMS well; (B) schematic illustration of the principle behind the chronoamperometric detection of H_2O_2 produced by living cells using an Os-HRP-modified ITO electrode.

concentration at a lower operational potential (Alpeeva et al., 2005; Ruzgas et al., 1996; Shleev et al., 2008; Crespilho et al., 2008, 2009). The sensitivity for the ROS detection with the electrochemical methods was found to be comparable with that with chemiluminescence methods (S. Kasai et al., 2005; Ashkenazi et al., 2009).

Osmium-polyvinylpyridine gel polymer containing HRP (Os-HRP), invented by Heller and coworkers (Vreeke et al., 1992), has been used for various biosensor elements (Garguilo and Michael, 1994; N. Kasai et al., 2005; Matsuura et al., 2005; Mizutani et al., 2008; Nakajima et al., 2003; Vreeke et al., 1992) because of its high sensitivity for the electrochemical detection of H_2O_2 at a lower operational potential. Electrodes modified with the polymer show high current densities, high sensitivity for H_2O_2, and low oxygen interference owing to effective electrical communication between the HRP (redox enzyme) and Os (electron transfer mediator) (Vreeke et al., 1992). Covalent attachment of the redox enzyme and electron transfer mediator to the electrode surfaces also allows the bioactivity of living cells to be reliably monitored, since attachment prevents signal degradation caused by the unexpected uptake of enzymes and mediators by cells. Heller et al. developed an Os-polyvinylpyridine gel polymer containing glucose oxidase (Os-Gox) for the fabrication of glucose-sensing devices. They implanted an Os-Gox-coated electrode into the subcutaneous tissue of a dog for in vivo glucose sensing (Linke et al., 1994). Os-HRP-modified microelectrodes have been used for the detection of choline in the extracellular fluid of rat brain (Garguilo and Michael, 1994) and for real-time imaging of H_2O_2 release from a rat hippocampal slice (N. Kasai et al., 2005).

We report here a new type of electrochemical device consisting of an Os-HRP-modified electrode chip and a polymer well for accommodating cells (Fig. 1A). The device was used to continuously monitor extracellular H_2O_2 released from granulocyte-like differentiated human promyelocytic leukemia HL-60 cells in the well. When the cells were stimulated with phorbol 12-myristate 13-acetate (PMA), the device indicated a significant increase in the amperometric response for H_2O_2 released from the cells (Fig. 1B). We compared amperometric responses with results from the luminol-based chemiluminescence method in the presence of NADPH oxidase inhivitor or ROS scavengers, in order to ensure that this device successfully detects extracellular H_2O_2 production.

2. Experimental

2.1. Materials and reagents

Ethanol, glucose, all-*trans* retinoic acid (RA), sodium luminol (NaLH), PMA, HRP and catalase (CAT) were purchased from Wako Pure Chemical Industries, Ltd. (Japan). RPMI 1640 medium, phosphate buffered saline (PBS) and SOD were purchased from Sigma Chemical Co. (St. Louis, MO, USA), and apocynin was purchased from Calbiochem (Germany). Aqueous solutions were prepared using high-purity distilled and deionized water from a Milli-Q filtration system (Millipore Corporation, USA).

2.2. Cell culture and differentiation

Human promyelocytic leukemia cell line HL-60, originally obtained from Riken Cell Bank (Japan), was maintained in RPMI 1640 medium supplemented with 10% fetal bovine serum (FBS; Hyclone, USA) and 1% penicillin–streptomycin (Invitrogen) in a humidified atmosphere containing 5% CO_2 (Kasai et al., 2006). To induce the differentiation of HL-60 cells to granulocyte-like cells, cells were incubated with 1.0 μM RA for 5 days. A 10 mM RA/99.5% ethanol stock solution was stored at −80 °C. A small aliquot of this solution was added to the growth medium to obtain the desired final concentration of RA, and to lower the ethanol concentration in the medium to eliminate undesired influences on the differentiation and proliferation of HL-60 cells. The differentiated cells were washed and resuspended in PBS supplemented with 1.0 mM glucose (PBS + Glu) for chemiluminescence and electrochemical measurements. The population of living cells was quantified with fluorescence microscopy (IX71; Olympus) using a fluorescent dye, calcein-AM (Dojindo Laboratories, Japan), and the cell suspensions were stored on ice until use.

2.3. Fabrication of PDMS well/Os-HRP ITO device

Fig. 1A shows a photograph of the electrochemical device used in this study. Indium-tin-oxide (ITO) coated glass (1.5 cm × 5.0 cm; Sano Vacuum Industries Co., Ltd., Japan) was cleaned in an oxygen plasma generator (LTA-101, Yanaco Co., Japan) for 30 s. Then, a 1.5-μL aliquot of Os-HRP polymer solution (Bioanalytical Systems, USA) was dropped on the ITO surface. The solution spread over the hydrophilic surface and formed a circular thin film approximately 4.5 mm in diameter after drying at 4 °C overnight. The coated electrode chips were stored at 4 °C in the dark.

For the cell assay, a poly-dimethyl siloxane (PDMS) well/Os-HRP ITO device was fabricated as follows. A PDMS prepolymer (SILPOTW/C, Dow Corning Toray, Japan) was poured on an acrylic master plate and cured in an oven at 90 °C for 30 min, then the PDMS replica was peeled off from the master. The resultant PDMS replica with a cylindric hole (5.0 mm diameter and 5.0 mm height) was placed on the electrode chip and used as a well to accommodate the cells. The PDMS well/Os-HRP ITO device thus fabricated was used for electrochemical monitoring of ROS released from the cells.

In order to confirm the catalytic function of HRP in the polymer layer, we prepared a comparable device but with deactivated HRP. Deactivation was achieved by treating the Os-HRP polymer layer with 15% H_2O_2 for 30 min at room temperature.

2.4. Equipment and methods for electrochemical measurement

All electrochemical measurements were performed using a potentiostat (HSV-100; Hokuto Denko Corp., Japan). Potentials were referenced to an Ag/AgCl sat. KCl electrode, using a gold wire as the counter electrode.

For basic characterization of the electrode chip, a portion of the chip with Os-HRP layer was soaked in 4.5 mL PBS solution. Cyclic voltammetry was conducted at a scan rate of 20 mV/s from −0.1 to +0.6 V at room temperature. Amperometric measurements for calibration of the H_2O_2 signal were performed at an operational potential of 0.0 V; after the current reached steady state at 0.0 V (i.e., almost all the Os was reduced to Os(II)), a 500-μL aliquot of serially diluted H_2O_2 standard solution (Cell Technology Inc., USA) was added to the gently stirred PBS solution containing the chip, and the current transient was monitored.

For the cell assay, the PDMS well/Os-HRP device was maintained at 37 °C on a thermo plate (Tokai Hit, Japan) during preincubation and measurements. Cell suspension (90 μL) containing 1×10^5 cells in PBS + Glu was added to the PDMS well, then a potential of 0.0 V was applied to the ITO electrode. After 10 min incubation, the current reached steady state. Then, a 10-μL aliquot of PMA/PBS-Glu solution was added to the well and the current transient was monitored.

In experiments conducted using NADPH oxidase inhibitor and ROS scavengers, 100 μM apocynin, 250 U/mL SOD or 250 U/mL CAT was added to the cell suspension in a well and incubated for 10 min before PMA stimulation.

2.5. Equipment and methods for chemiluminescence measurements

Chemiluminescence measurements were performed using a highly-sensitive CCD camera (PI-MAX 512RB; Princeton Instruments, USA) placed 30 cm above a sterile black polystyrene 96-well cell culture plate (Nunc) containing samples in a shade box. The 96-well plate was set on a thermo plate (Tokai Hit, Japan) to keep the samples at 37 °C. Cell suspension (150-μL aliquots containing 2×10^5 cells in PBS + Glu) was dispensed into the wells and incubated on the thermo plate for 10 min. Chemiluminescence measurements were started within 5 min of adding a 50-μL aliquot of 37 °C pre-warmed stimulus mixture solution containing PMA, 4 mM LHNa and 16 U/mL HRP in PBS-G. Chemiluminescence images were accumulated for 5 or 15 min. For time course monitoring, chemiluminescence intensities of the images were calculated as total intensities of 40×40 pixels trimed around each well. In experiments conducted using NADPH oxidase inhibitor and ROS scavengers, 100 μM apocynin, 250 U/mL SOD or 250 U/mL CAT was added to the cell suspension in a well and incubated for 10 min before PMA stimulation.

3. Results and discussion

3.1. Characterization of the electrode chip

We performed cyclic voltammetry and amperometry to characterize the basic performance of an Os-HRP-modified ITO electrode without PDMS well and cells. The cyclic voltammogram showed symmetric oxidation and reduction waves without diffusion tails at the potential of 0.36 V. The shapes were consistent with that reported in previous paper (Vreeke et al., 1992). The peak currents increased linearly with the scan rate in the range 4–100 mV/s. These phenomena are typical for surface-confined redox species. The surface concentration of the redox site (Os complex) was calculated from a coulometric analysis of the peaks, and was found to be 7.5×10^{-9} mol/cm^2. The cyclic voltammogram with deactivated HRP was similar to that with active HRP, indicating that the deactivation process does not significantly affect the redox performance of the Os complex. We also observed the chronoamperometric response of the Os-HRP (active)-modified electrode chip at 0.0 V for the successive addition of 1.0 μM H_2O_2 with stirring. On each addition of H_2O_2, the reduction current immediately increased, and then reached steady-state within 10 s. The response current at steady-state increased with increasing concentration of H_2O_2 in the solution. On the other hand, the electrode chip with deactivated HRP showed no response upon addition of H_2O_2. This clearly suggests that treating the electrode chip with 15% H_2O_2 for 30 min completely deactivates the HRP in the polymer, and that H_2O_2 is not directly oxidized or reduced on the electrode surface at 0.0 V even if the Os polymer is confined on the surface.

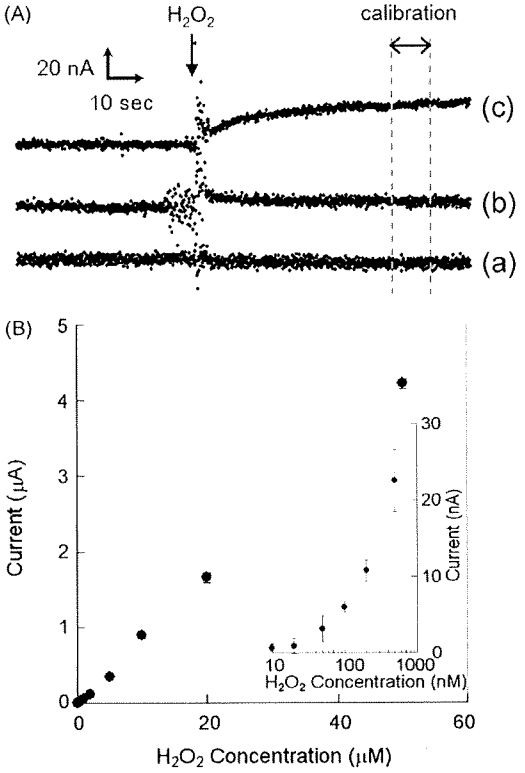

Fig. 2. (A) Typical amperometric response of the electrode chip for standard H_2O_2 solutions at low concentrations. Amperometric measurements were carried out at +0.0 V vs. an Ag/AgCl reference electrode. The concentration of H_2O_2: (a) 0 nM, (b) 50 nM, (c) 500 nM. (B) Calibration curve for the averaged amperometric responses at 50–60 s in (A) against the concentration of H_2O_2. *Inset*: The low concentration part of the calibration curve. Error bars show ±standard deviation ($n = 3$). The coefficient of variations for over 1 μM H_2O_2 were within 10%.

Fig. 2A shows the chronoamperometric responses at low H_2O_2 concentrations. Although the solution stirring caused data scattering, a clear increase in the reduction current was observed after injection of H_2O_2 even at 50 nM H_2O_2. We measured the average currents between 50 and 60 s after H_2O_2 injection to obtain the calibration curve for determining H_2O_2 concentration (Fig. 2B). The reduction current increased linearly with H_2O_2 concentration in the range of 50 nM to 50 μM. The detection range is in good agreement with that reported in a previous study that used a 3-mm carbon disc electrode coated with the same polymer (Vreeke et al., 1992) and also indicates that our device can conduct highly sensitive H_2O_2 detection compared with other electrochemical techniques (Ruzgas et al., 1996).

3.2. Electrochemical and chemiluminescence signal transients in cell measurements depending upon PMA concentration

Using the PDMS well/Os-HRP ITO device, we monitored the electrochemical signal transient originating from ROS released from RA-differentiated HL-60 cells stimulated by various concentrations

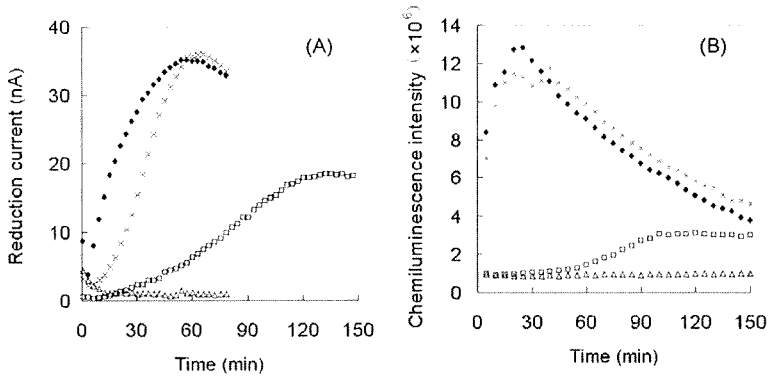

Fig. 3. Typical PMA concentration-dependent time course variation in chronoamperometric responses (A) and chemiluminescence intensities (B). The concentrations of PMA were (●) 10 μg/mL, (×) 1 μg/mL, (□) 0.1 μg/mL, and (△) without PMA. Chemiluminescence intensities were calculated for total intensities of 40 × 40 pixels from 5 min accumulated images. Gain: 250.

of PMA. Fig. 3A shows typical chronoamperometric responses: the reduction currents gradually increased after PMA (0.01–10 μg/mL) was added to the well, and then declined after a period of time. The time required to show the current peak, and the response intensity, tends, respectively, to be shorter and larger as the concentration of PMA for cell stimulation increased. No significant current change was observed without PMA. Fig. 3B shows the time course of chemiluminescence intensities under the same conditions as the electrochemical measurements. The two techniques provide similar results, confirming that the PDMS well/Os-HRP ITO device affords reliable information on ROS production by differentiated HL-60 cells.

3.3. Characterization of the electrochemical signal

To characterize the electrochemical signals, we investigated the effect of apocynin (NADPH oxidase inhibitor), SOD (scavenger of $^{\bullet}O_2^-$) and CAT (scavenger of H_2O_2). HL-60 cells were preincubated in the PDMS well/Os-HRP ITO device with the scavenger or inhibitor. After 10 min preincubation, the cells were stimulated with 1 μg/mL PMA and the reduction current was monitored. Fig. 4A shows the chronoamperometric response under a variety of conditions. The increase in the reduction current in the presence of 100 μM apocynin (Fig. 4A(b)) was less than 20% of that observed in the control experiment (Fig. 4A(a)). This result indicates that more than 80% of the current response originates from the reaction catalyzed by NADPH oxidase:

$$NADPH + 2O_2 \xrightarrow{\text{NADPH oxidase}} NADP^+ + 2{}^{\bullet}O_2^- + H^+ \quad (1)$$

We also employed SOD and CAT as scavengers of $^{\bullet}O_2^-$ and H_2O_2, respectively. SOD catalyzes the dismutation of $^{\bullet}O_2^-$ into O_2 and H_2O_2:

$$2{}^{\bullet}O_2^- + 2H^+ \xrightarrow{\text{SOD}} O_2 + H_2O_2 \quad (2)$$

When SOD is added to the cell suspension, the reduction current is expected to increase because additional H_2O_2 would be produced by reaction (1). On the other hand, CAT is expected to reduce the reduction current because it catalyzes the decomposition of hydrogen peroxide into and O_2 and H_2O:

$$2H_2O_2 \xrightarrow{\text{CAT}} 2H_2O + O_2 \quad (3)$$

In the presence of 250 U/mL SOD, the reduction current increased immediately after addition of PMA (Fig. 4A(c)), whereas incubation with 250 U/mL CAT suppressed the current increase (Fig. 4A(d)) compared with the control experiment (Fig. 4A(a)). No obvious increases in the reduction current were observed when PMA stimulation was omitted (Fig. 4A(e)), when undifferentiated HL-60 cells with no ROS generation activity (Muranaka et al., 2005) were used (Fig. 4A(f)), or when the device was prepared with deactivated HRP (Fig. 4A(g)). All the above findings indicate that H_2O_2 is the main molecule responsible for the generation of the electrochemical signal by leucocytes.

The initial production rate of H_2O_2 was determined from the initial slope of the current response using the H_2O_2-reduction current response curve shown in Fig. 4A. The initial production rate of H_2O_2 in the presence of 250 U/mL SOD is more than 3 times

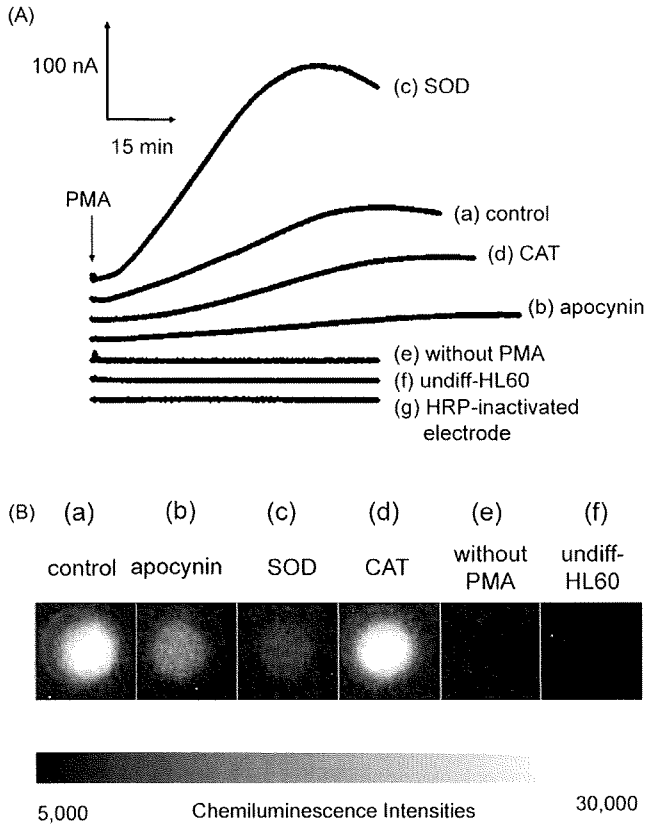

Fig. 4. Typical amperometric response transients (A) and accumulated chemiluminescence images of 30–45 min (B) after stimulation with 1 μg/mL PMA; (a) control, (b) with 100 μM apocynin, (c) with 250 U/mL SOD, (d) with 250 U/mL CAT, (e) without PMA, (f) using undifferentiated HL-60 cells and (g) using an HRP-deactivated electrode.

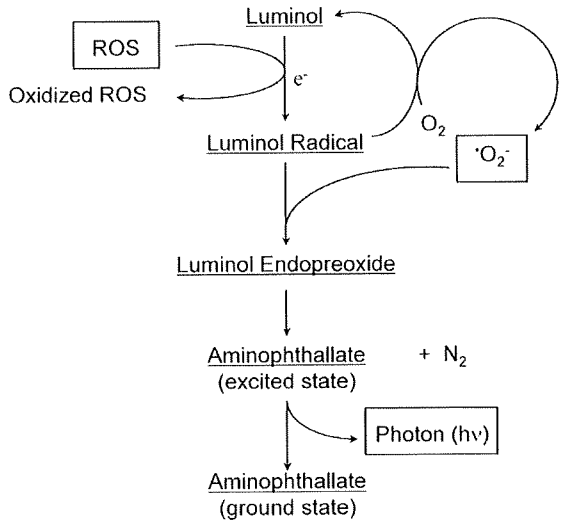

Fig. 5. Scheme of the chemical reaction pathway leading to luminol dependent chemiluminescence with ROS.

larger than that observed in the control measurement. On the other hand, 250 U/mL CAT decreased H_2O_2 production by two-thirds. These results are in good agreement with the predictions based on reactions (2) and (3). H_2O_2 production rates between 10 and 30 min after PMA stimulation were found to be approximately 6, 18 and 4 pmol/min per 1×10^5 cells for without scavenger, with SOD, and with CAT, respectively. The production rates determined in the present study are considerably lower than those reported by Umegaki and Fenech (2000). They reported that granulocyte-like-differentiated HL-60 cells stimulated with 60 ng/mL PMA produced H_2O_2 at 100 pmol/min (phenol red method) and $^{\bullet}O_2^-$ at 300 pmol/min (cytochrome c method) per 1×10^5 cells. Although the reason for the discrepancy is not clear at present, the ratio of the rate with SOD to that without SOD in the present study is 3, which is a reasonable range because 1/2 mol of H_2O_2 is produced from 1 mol of $^{\bullet}O_2^-$ in the presence of SOD (Eq. (2)). For comparison, the ratio reported by Umegaki and Fenech (2000) is 2.5.

3.4. Comparison of chemiluminescence and electrochemical methods

Fig. 4B shows chemiluminescence images of wells with 2×10^5 HL-60 cells under the conditions as the electrochemical measurements in Fig. 4A. The images were obtained 30–45 min after stimulation with 1 μg/mL PMA (15 min accumulated images). Incubation with 100 μM apocynin decreased the chemiluminescence signal (Fig. 4B(b)), and no chemiluminescence was detected from HL-60 cells without PMA stimulation or from undifferentiated HL-60 cell with PMA stimulation. These results agree with those from electrochemical measurements using the PDMS well/Os-HRP ITO device. However, incubations with SOD and CAT gave different results from those obtained electrochemically: the presence of 250 U/mL SOD effectively decreased chemiluminescence (Fig. 4B(c)), and 250 U/mL CAT did not affect the signal (Fig. 4B(d)). The present assay is based on detection of luminol-dependent chemiluminescence, which is also predominantly derived from $^{\bullet}O_2^-$ in respiratory burst (Dahlgren and Karlsson, 1999; S. Kasai et al., 2005). Ashkenazi et al. (2009) reported that 300 U/mL SOD inhibits 90% of isoluminol chemiluminescence activity, but more than doubles the electrochemical signal for H_2O_2. This difference is clearly explained by the reaction mechanisms: electrochemical measurements detect the H_2O_2 produced from the SOD-catalyzed dismutation of $^{\bullet}O_2^-$ (Eq. (2)), whereas the luminol-based chemiluminescence reaction has critical step intermediated by $^{\bullet}O_2^-$ (Fig. 5) (Li et al., 1999). SOD decreases the concentration of $^{\bullet}O_2^-$, thereby reducing chemiluminescence. Electrochemical detection is thus effective for monitoring extracellular H_2O_2, while the chemiluminescence method is suitable for real-time monitoring of ROS generation by cells. H_2O_2 is a key metabolite in oxidative stress and is important in cell signaling cascades (Liu and Zweier, 2001). Thus, a sensing system for monitoring extracellular H_2O_2 is very useful for disclosing oxidative stresses and other intracellular processes. The present device, based on the electrochemical detection of H_2O_2, has advantages for sensitivity, selectivity and quantitation, and will be applicable for a variety of studies dealing with living cells.

4. Conclusion

In this study, we developed an electrochemical device for continuous monitoring extracellular H_2O_2. The device consists of an Os-HRP-modified electrode chip for highly sensitive H_2O_2 detection and a PDMS well for the accommodation of living cells. When granulocyte-like-differentiated HL-60 cells in the well were stimulated with PMA, amperometric responses on the Os-HRP polymer-modified electrode chip were generated, indicating ROS production by the cells. SOD increased the electrochemical response, CAT decreased the response, and apocynin significantly decreased the response. All of these responses can be explained by the intrinsic functions of these species. The results indicate that H_2O_2 is the main molecule contributing to the generation of the electrochemical signal. The present electrochemical detection device is a useful tool for continuous monitoring of H_2O_2 release in respiratory burst and also can be applied to simple and portable whole-cell biosensing systems for inflammatory compounds, and for hazardous materials causing oxidative stresses (Inoue et al., 2008).

Acknowledgements

This work was partly supported by a Grant-in-Aid for Scientific Research (S) (No. 18101006) from the Japan Society for the Promotion of Science (JSPS) and Special Coordination Funds for Promoting Science and Technology, Formation of the Innovation Center for Fusion of Advanced Technologies from the Japan Science and Technology Agency.

Appendix A. Supplementary data

Supplementary data associated with this article can be found, in the online version, at doi:10.1016/j.bios.2009.12.014.

References

Alpeeva, I.S., Niculescu-Nistor, M., Leon, J.C., Csoregi, E., Sakharov, I.Y., 2005. Biosens. Bioelectron. 21, 742–748.
Amatore, C., Arbault, S., Bouton, C., Coffi, K., Drapier, J.C., Ghandour, H., Tong, Y.H., 2006. Chembiochem 7, 653–661.
Ashkenazi, A., Abu-Rabeah, K., Marks, R.S., 2009. Talanta 77, 1460–1465.
Crespilho, F.N., Ghica, M.E., Gouveia-Caridade, C., Oliveira, O.N., Brett, C.M.A., 2008. Talanta 76, 922–928.
Crespilho, F.N., Lanfredi, A.J.C., Leite, E.R., Chiquito, A.J., 2009. Electrochem. Commun. 11, 1744–1747.
Dahlgren, C., Karlsson, A., 1999. J. Immunol. Methods 232, 3–14.
Garguilo, M.G., Michael, A.C., 1994. Anal. Chem. 66, 2621–2629.
Griendling, K.K., Harrison, D.G., 1999. Circ. Res. 85, 562–563.
Hardy, S.J., Robinson, B.S., Poulos, A., Harvey, D.P., Ferrante, A., Murray, A.W., 1991. Eur. J. Biochem. 198, 801–806.
Inoue, K.Y., Yasukawa, T., Shiku, H., Matsue, T., 2008. Electrochemistry 76, 525–528.
Kasai, N., Han, C.X., Torimitsu, K., 2005. Sens. Actuators B Chem. 108, 746–750.
Kasai, S., Shiku, H., Torisawa, Y.S., Noda, H., Yoshitake, J., Shiraishi, T., Yasukawa, T., Watanabe, T., Matsue, T., Yoshimura, T., 2005. Anal. Chim. Acta 549, 14–19.

Kasai, S., Shiku, H., Torisawa, Y.S., Nagamine, K., Yasukawa, T., Watanabe, T., Matsue, T., 2006. Anal. Chim. Acta 566, 55–59.
Li, Y.B., Zhu, H., Trush, M.A., 1999. Biochim. Biophys. Acta 1428 (1), 1–12.
Linke, B., Kerner, W., Kiwit, M., Pishko, M., Heller, A., 1994. Biosens. Bioelectron. 9, 151–158.
Liu, X.P., Zweier, J.L., 2001. Free Radic. Biol. Med. 31, 894–901.
Lundqvist, H., Dahlgren, C., 1996. Free Radic. Biol. Med. 20, 785–792.
Matsuura, H., Sato, Y., Niwa, O., Mizutani, F., 2005. Anal. Chem. 77, 4235–4240.
Mizutani, F., Ohta, E., Mie, Y., Niwa, O., Yasukawa, T., 2008. Sens. Actuators B Chem. 135, 304–308.
Muranaka, S., Fujita, H., Fujiwara, T., Ogino, T., Sato, E.F., Akiyama, J., Imada, I., Inoue, M., Utsumi, K., 2005. Antioxid. Redox Signal. 7, 1367–1376.
Nakajima, K., Yamagiwa, T., Hirano, A., Sugawara, M., 2003. Anal. Sci. 19, 55–60.
Radi, R., Cosgrove, T.P., Beckman, J.S., Freeman, B.A., 1993. Biochem. J. 290, 51–57.
Rossi, F., 1986. Biochim. Biophys. Acta 853, 65–89.
Ruzgas, T., Csoregi, E., Emneus, J., Gorton, L., MarkoVarga, G., 1996. Anal. Chim. Acta 330, 123–138.
Shleev, S., Wettero, J., Magnusson, K.E., Ruzgas, T., 2008. Cell Biol. Int. 32, 1486–1496.
Stefanska, J., Pawliczak, R., 2008. Mediators Inflamm. 2008, 1–10.
Umegaki, K., Fenech, M., 2000. Mutagenesis 15, 261–269.
Vreeke, M., Maidan, R., Heller, A., 1992. Anal. Chem. 64, 3084–3090.

Electrochemical characterization of enzymatic activity of yeast cells entrapped in a poly(dimethylsiloxane) microwell on the basis of limited diffusion system

Hitoshi Shiku,*[a] Shun Goto,[a] Sungbong Jung,[a] Kuniaki Nagamine,[a] Masahiro Koide,[b] Tomosato Itayama,[b] Tomoyuki Yasukawa[c] and Tomokazu Matsue*[a]

Received 19th May 2008, Accepted 2nd September 2008
First published as an Advance Article on the web 20th October 2008
DOI: 10.1039/b808428a

A highly sensitive and quantitative analysis was performed using a poly(dimethylsiloxane) (PDMS) microwell array in a scanning electrochemical microscopy setup. A microelectrode with a relatively large seal radius was used to cover the top of the cylindrical PDMS microwell (96 pL). The voltammogram for 4 mM ferrocyanide resulted in a charge value of 38 nC, suggesting that almost 100% of the reductant in the microwell was converted to the oxidation current. When genetically modified yeast cells were entrapped in the microwell, the accumulation of *p*-aminophenol (PAP) produced by expressing β-galactosidase (βGAL) was successfully observed.

1. Introduction

Analytical chemistry within small volumes has shown significant impacts to explore new research fields including single-cell analysis[1–6] and single molecule dynamics.[7,8] Various micro- and nanostructures were constructed and combined with highly sensitive detection systems based on optical and electric amplifiers for the purpose of simplifying sample preparation, shortening the time per assay, and elevating the throughput of the analysis. Among these micro- and nanostructures, poly(dimethylsiloxane) (PDMS) microchamber arrays[7,9] or microchannels[8,10–12] are probably the most simple and flexible devices that can be used as lab-on-a-chip devices.

The electrochemical measurement system is also possible to realize parallel and rapid assays with a small-volume microwell array.[13] However, electrochemical studies of small-volume samples require at least two electrodes to maintain the entire electric circuit connected during the measurements.[14–23] Therefore, the electrode must be designed inside the microchamber[14–19] or inserted into the small space under a micromanipulator operation.[20–23] In the experimental setup based on scanning electrochemical microscopy (SECM),[24,25] however, it is relatively easy to form a confined ultra-small volume.[26–28] The electrochemical behavior of the microelectrode observed in the microchamber is drastically different from that observed when the electrode is placed in the bulk solution. In the present study, we combined the SECM technology with the PDMS cylindrical microwell array to quantitatively evaluate the enzymatic activity of recombinant yeast cells expressing β-galactosidase (βGAL). As a model system, a yeast-two-hybrid strain was selected because it is widely used not only for screening protein–protein interactions but also for detecting environmental pollutants.[5,6,29–36] Schwartz–Mittelman *et al.* demonstrated the electrochemical evaluation of the estradiol activities of various compounds by using human estrogen receptor-alpha.[31–32]

The accumulated product from the yeast cells in the microwell is converted to electric charge. The enzymatic activity of the yeast cells in the confined system is quantitatively analyzed and compared with that in the open system based on the spherical diffusion theory. We find that the cellular activity is strongly affected by the designs of the microchamber and detection system. The confined PDMS microwell system allows the accumulation of the product, and therefore, is advantageous for highly sensitive analyses. However, we must be careful to discuss the enzymatic activity and mass transfer rate in small volume analysis because these parameters might change depending on the environmental conditions.

2. Materials and methods

2.1 Reagents

The (100) silicon monocrystal wafer (thickness: 230 μm, optically polished on both sides) was purchased from SUMO Co., Tokyo, Japan. The negative photoresist, SU-8-3050, was purchased from Microchem Co. USA. PDMS (Sylgard 184) was purchased from Dow Corning, Co. USA. 17β-Estradiol was purchased from Sigma, USA. *p*-Aminophenyl-β-D-galactopyranoside (PAPG) was purchased from Tokyo Chemical Industry Co., Ltd., Japan. Triton X-100 was purchased from Polysciences, Inc., USA. Dimethyl sulfoxide (DMSO) and *p*-aminophenol (PAP) were purchased from Wako Pure Chemicals, Japan. All the solutions were prepared using distilled and deionized water purchased from Direct-Q (Millipore, USA).

2.2 Fabrication of the PDMS microwell array

The PDMS microwell array was fabricated by curing the prepolymer on the (100) Si substrate with a master. The master

[a]*Graduate School of Environmental Studies, Tohoku University, 6-6-11, Aramaki-Aoba, Sendai 980-8579, Japan. E-mail: shiku@bioinfo.che.tohoku.ac.jp; matsue@bioinfo.che.tohoku.ac.jp*
[b]*Environmental Chemistry Division, National Institute for Environmental Studies, 16-2 Onogawa, Tsukuba 305-8506, Japan*
[c]*Graduate School of Material Science, University of Hyogo, Hyogo, Japan*

 This journal is © The Royal Society of Chemistry 2009

was photolithographically patterned using the negative photoresist (SU-8 3050). A 10 : 1 mixture of the silicon elastomer and the curing agent was poured on the master and left at 80 °C for 1 h for curing the prepolymer. The PDMS replica was then peeled from the substrate. The diameter and depth of the PDMS microwell were both 50 μm.

2.3 Yeast strain and growth conditions

The yeast strain used in the present study was *Saccharomyces cerevisiae* Y190, donated by Dr Fujio Shiraishi from the National Institute for Environmental Studies. The expression plasmid contains the human estrogen receptor α (hERα),[31–35] instead of the medaka estrogen receptor α (medERα: *Oryzia latipes*),[29] fused with GAL4 DBD (binding domain). The plasmid containing coactivator TIF2 fused with the GAL4 activation domain (GAL4 AD) was also introduced into the yeast cells carrying the β-galactosidase reporter gene.[33,34] The cells were preincubated for 24 h at 30 °C with shaking at 100 rpm in a modified Sabouraud dextrose (SD) medium (without tryptophan and leucine).

The cell suspension (60 μL) was then mixed with the medium (60 μL) containing 10 nM 17β-estradiol and 2.0% (v/v) DMSO, and incubated for 4 h at 30 °C with shaking at 100 rpm to induce the β-galactosidase expression. The medium was exchanged to a 80 μL of Z-buffer (60.0 mM $Na_2HPO_4 \cdot 12H_2O$, 39.7 mM $NaH_2PO_4 \cdot 2H_2O$, 10.0 mM KCl, 10.0 mM $MgSO_4 \cdot 7H_2O$; pH 7.0) including 0.3% (v/v) Triton X-100, a nonionic surfactant to incubate for 1 h at 30 °C with shaking at 100 rpm (final concentration of the yeast cells was 1×10^7 cells mL^{-1}).

2.4 Electrochemical detection of β-galactosidase activity in yeast cells

The PDMS microwell array was irradiated with O_2 plasma at 100 W for 1 min in order to make the surface of the well hydrophilic. Generally, the O_2 plasma treated PDMS surface maintains the sufficient hydrophilic nature for 1 h to smoothly introduce aqueous solutions within the microwell array. Under aqueous solution, however, the hydrophilic nature of the O_2 treated PDMS surface is maintained for at least 12 h.The yeast cell suspension (100 μL) was first dispensed on the PDMS microwell array and stabilized for 10 min. Then, the suspension was withdrawn using a filter paper to remove the excess yeast cells present on the outer surface of the microwell. The liquid and yeast cells remained the inside the PDMS wells only. Secondary, the measuring solution was further poured on the PDMS microwell array gently. For the electrochemical measurements, the PDMS microwell array containing the yeast cells was carefully soaked in the Z-buffer solution containing 7.4 mM PAPG and 0.3% Triton X-100. The concentration of Triton X-100 in the measuring solution was determined to optimize the activity of the yeast cells. The mass-transfer of PAPG and PAP through the cellular membranes was sufficiently promoted, but βGAL still remained in the yeast cells. In this study, the number of cells in the PDMS microwell was controlled to be less than 150 so that the yeast cells remain at the bottom (50 μm ∅) of the cylindrical PDMS microwell at monolayer level. The exact number of cells in the well was manually counted from the photograph recorded for each microwell in which the electrochemical measurement was performed.

The electrochemical measurement was carried out using an SECM system including a potentiostat (HA1010mM8; Hokuto Denko Corp., Tokyo, Japan), an inverted microscope (Nikon diaphot T200), and a motor-driven XYZ stage (Chuo-Seiki M9103). An Ag/AgCl-saturated KCl electrode was used as the reference/counter electrode. A Pt-microelectrode (radius: 10 μm; radius of the tip including the insulator part: 85 μm) was used as the working electrode. The β-galactosidase (βGAL) activity expressed in the yeast cells was monitored by detecting the oxidation current for PAP, a product of the enzyme-catalyzed hydrolysis of PAPG inside the trapped cells.[29–32,37–40] The electrochemical experiment was performed on a 4–6 cm^2 -piece of the PDMS microwell array sheet set in a disposable 60 mm-diameter culture dish. The Ag/AgCl reference electrode was set on the PDMS microwell array sheet. The distance between the working and the reference electrode was about 10–20 mm. In the case that the glass seal part of the working electrode completely covers the PDMS microwell, electrochemical measurement is not available because current does not flow. However, we have recognized that there is an electric connection due to leakage of the ionic flow between the working and the reference electrodes even when reactant within the microwell was consumed almost 100%.

3. Results and discussion

Fig. 1(a) shows the schematic illustration of the experimental setup. The top opening of the PDMS cylindrical microwell is covered with the disk plane of a working microelectrode tip to accumulate PAP produced by βGAL in the yeast cells. The time period between the covering of the PDMS microwell with the microelectrode tip and the application of the potential was defined as the accumulation time, t_{accu}. As t_{accu} increases, the concentration of PAP in the microwell also increases. After maintaining the tip potential at 0.0 V for t_{accu}, the potential was stepped to +0.3 V to oxidize PAP accumulated in the microwell. The product of the PAP oxidation is quinone imine (QI). Fig. 1(b) shows an optical micrograph of the PDMS microwell array. The height of the SU-8 mold of the PDMS microwell was 50 ± 1 μm measured with a surface profiler. The diameter of the microwell was 50 ± 1.3 μm under the optical microscopic observation.

Prior to the measurements using the yeast cells, the electrochemical behavior in the confined microwell was characterized by cyclic voltammetry. Fig. 2 shows the cyclic voltammograms (CVs) of 4.0 mM $K_4Fe(CN)_6$/0.1 M KCl in the PDMS microwell. CVs shown in the present study were performed at scan rate of 20 mV s^{-1}. The microelectrode was positioned at various heights (z) from the upper surface of the PDMS microwell (+300 to −100 μm). The point at $z = 0$ defines the position where the tip touches the upper surface of the PDMS microwell. The negative z value does not reflect the actual z-position of the tip, but indicates that the microelectrode pushes down the top of the PDMS microwell. According to the spherical diffusion theory, when the microelectrode tip is sufficiently far from the upper surface of the PDMS microwell (z = +300 μm), the CV has a typical sigmoidal shape, and the oxidation current for $Fe(CN)_6^{4-}$ reaches the

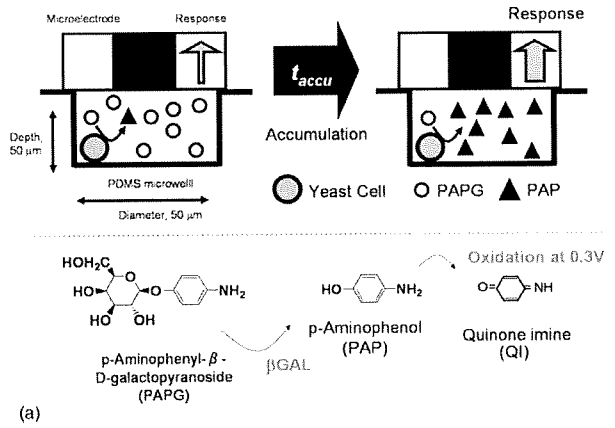

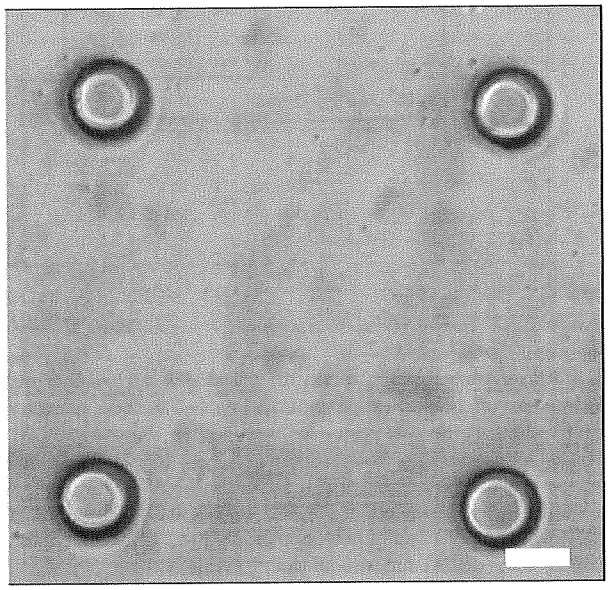

(b)

Fig. 1 (a) Schematic illustration of the experimental setup. The top of the PDMS cylindrical microwell (diameter: 50 μm; depth: 50 μm) is covered with the disk plane of a working microelectrode tip to accumulate the PAP produced by the βGAL in the yeast cells. The accumulation time was defined as t_{accu}. After maintaining the tip potential at 0 V for t_{accu}, the potential was stepped to +0.3 V to oxidize the PAP accumulated in the microwell. Schemes of the enzymatic and electrochemical reaction were also showen. (b) Photograph of the PDMS micriowell array. Bar, 50 μm.

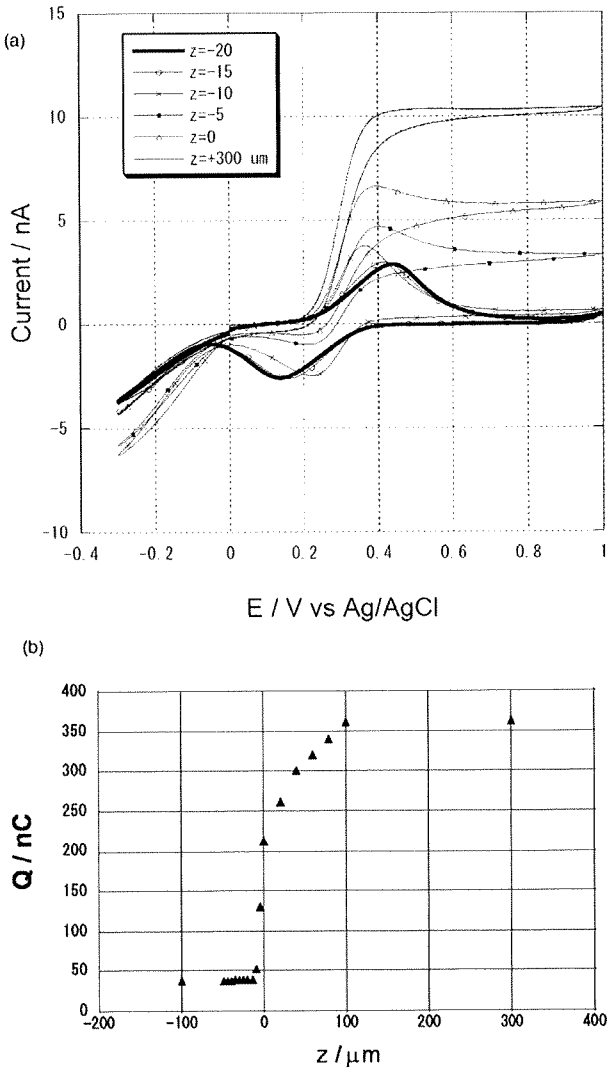

Fig. 2 (a) Cyclic voltammograms in 4 mM $K_4Fe(CN)_6$/0.1 M KCl for the PDMS microwell. Scan rate: 20 mV s^{-1}. The microelectrode was located at various z-positions (+300 to −20 μm). The point at $z = 0$ was defined as that where the tip touched the top of the PDMS microwell. (b) Plot of the electric charge *versus* z (+300 to −100 μm). Tip radius: 10.5 μm; Insulator radius: 85 μm.

steady state in the positive potential region. The shape of the voltammogram drastically changed at $z = 0$, showing an oxidation peak at +0.4 V due to the limited diffusion. For z values less than −10 μm, the oxidation current in the positive potential region (more positive than +0.7 V) was found to become almost zero, indicating that $Fe(CN)_6^{4-}$ in the microwell was almost completely consumed. When the potential was scanned in the negative direction, a reduction peak was observed at +0.15 V. The reduction current observed in less than −0.05 V originates from the oxygen dissolved in the solution.[12,42] The relatively large peak separation of 0.35 V is mainly due to the solution resistance, which depends on several parameters of the experimental setup, including the seal size of the tip electrode and the position of the tip (z). The electric charges estimated from the areas under the oxidation and reduction peaks were 38 and 32 nC, respectively.

Fig. 2(b) shows the plot of the electric charge of the oxidation peak as a function of z. The charge was almost constant (38.22 ± 0.143 nC) when the z value was less than −15 μm. This result suggests that the confined volume (96 pL) in the present experimental setup is preserved, regardless the position of the microelectrode tip in the relatively wide range, $z = -15$ to −100 μm. Therefore, we can precisely analyze the electrochemical behavior in the small volume of the confined cavity formed with the PDMS microwell and microelectrode cap. In this article, the electrochemical measurements for the yeast cells entrapped in the PDMS microwell were performed at $z = -30$ μm. The

This journal is © The Royal Society of Chemistry 2009

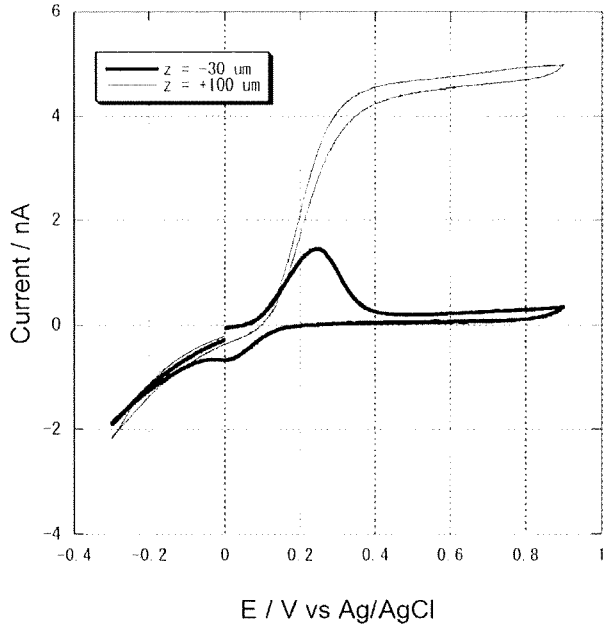

Fig. 3 Cyclic voltammograms in 0.82 mM PAP/Z-buffer for the PDMS microwell. Scan rate: 20 mV s^{-1}. The microelectrode was located attaching ($z = -30$ μm) or far from the PDMS microwell ($z = +100$ μm). Tip radius: 12 μm.

experimental setup we introduce here requires a probe positioner but need not control the vertical position with less than 10 μm preciseness. Since the microwell is made of a PDMS elastomer, the tip and microwell are less likely to damage, and therefore, both can be used repeatedly. There exist many other methods for carrying out small-volume electrochemistry using paraffin oil,[21,23] mercury,[28] oil/water droplets,[19,22] or various microfabricated 3D structures.[14–18] The present method utilizing the PDMS microwell has great advantages from the viewpoints of cost, simplicity, reproducibility, and throughput. The CV of 0.82 mM PAP oxidation within the microwell was also performed and shown in Fig. 3. At +0.3 V, the PAP oxidation current could be obtained whereas PAPG not oxidized.[29,41] The charge for the PAP oxidation 14.9 ± 0.95 nC ($n = 8$) was in good agreement with the expected theoretical value 15.3 nC in the confined microwell of 96 pL. The CV behaviours of the PAP for near ($z = -30$ μm) and far from the PDMS ($z = +100$ μm) are basically the same tendencies as those of the $K_4Fe(CN)_6$ system, however, when the potential was scanned back in the negative direction, a reduction peak was small at $z = -30$ μm probably because the product from the PAP oxidation, QI was not chemically stable.

Next, we quantitatively determined the amount of PAP produced by βGAL in the yeast cells. Fig. 4 shows the results of the chronoamperometry on the PDMS microwell entrapping 144 yeast cells. Before the potential was stepped from 0 V to +0.3 V to detect PAP, the microelectrode tip was positioned to cover the top of the PDMS microwell for different accumulation times (t_{accu} = 1–31 min), and the current responses obtained without the yeast cells (t_{accu} = 1, 11 min) were recorded. The current responses obtained with the yeast cells were considerably larger than those obtained without the yeast cells. We calculated the

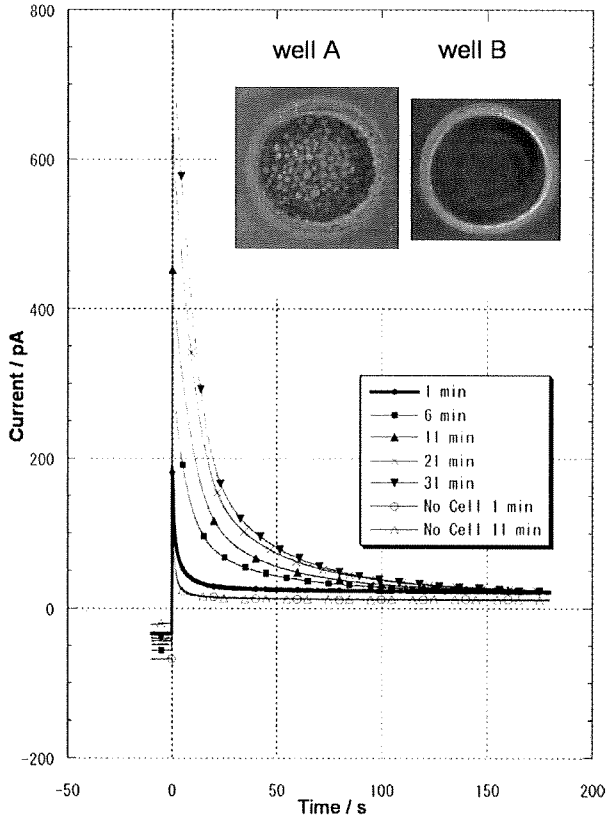

Fig. 4 Chronoamperometric results for the PDMS microwell entrapping 144 yeast cells. Before the potential was stepped from 0 V to +0.3 V, the microelectrode tip was positioned to cover the top of the PDMS microwell for various t_{accu}, from 1 to 31 min (t_{accu} = 1, 6, 11, 21, 31 min). The same procedures were also performed for the PDMS well without the yeast cells. Measuring solution: 7.4 mM PAPG, 0.3% Triton-X100T, Z-buffer. Tip radius: 12 μm. Inset: photograph of the PDMS microwells measured with (well A) and without (well B) yeast cells.

electric charge and time integration of the current to quantitatively evaluate the βGAL activity. The charges obtained for t_{accu} = 1 min and 11 min are approximately 5 nC and 11 nC, respectively. The 6 nC increase in the charge during the accumulation time clearly indicates that PAP is produced by the βGAL activity in the yeast cells, and is accumulated in the PDMS microwell within 10 min. When yeast cells do not exist, the background charge was independent of t_{accu}. The baseline current at 0 V fluctuated between −95 and −145 pA ($n = 12$, data not shown), probably due to the reduction in the concentrations of the dissolved oxygen and PAPG;[40] however, the background charges recorded at the +0.3 V potential step was almost constant (~3 nC). This low background charge is probably due the oxidation of PAP produced from PAPG *via* chemical (nonenzymatic) hydrolysis in solution.

Fig. 5 and 6 show the plots of the electric charge and enzymatic activity, respectively, as a function of t_{accu}. The measurements were performed three times, and the standard deviation (SD) was 2.2 to 7.8% of the each average value. The electric charge was converted to the βGAL activity (PAP product/mol s^{-1} $cell^{-1}$) by using the reaction electron number for PAP ($n_{ET} = 2$) and the Faraday constant (96500 C mol^{-1}). Fig. 5 illustrates that the

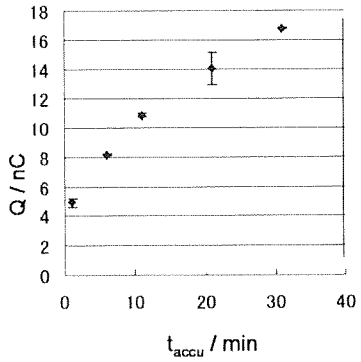

Fig. 5 Plot of the electric charge *versus* t_{accu}. The measurement was performed thrice under each set of experimental conditions ($n = 3$).

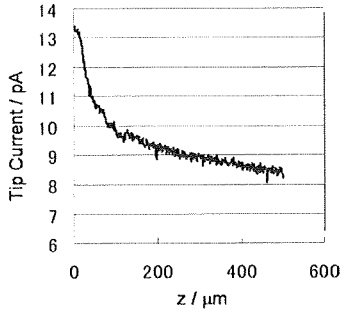

Fig. 7 Oxidation current profile as a function of the height (z) from the top of the PDMS well entrapping 86 yeast cells recorded at the center of the well in the measuring solution of 7.4 mM PAPG, 0.3% Triton-X100T, Z-buffer. Tip scan rate: 9.8 μm s^{-1}; Tip potential: +0.3 V *vs.* Ag/AgCl; Tip radius: 12 μm.

accumulation of PAP in the pL level of small volume chamber has been successfully detected. However, it should be noted that the PAP accumulation rate is not liner to t_{accu} and that the βGAL activity deceases with t_{accu} as shown in Fig. 6.

This type of confined PDMS microwell system allows another electrochemical analysis categorized in a steady-state method. In Fig. 4, the oxidation current for the microwell with 144 yeast cells is greater than that for the microwell without yeast cells by 11 pA, even 150 s after the potential step. This phenomenon implies that the rate of PAP production by yeast cells is equal to the rate of oxidation of PAP at the microelectrode, and the overall processes in the microwell reach the steady state. Under these circumstances, the βGAL activity can also be evaluated from the steady-state oxidation current; this value was found to be 3.96×10^{-19} mol s^{-1} $cell^{-1}$, which corresponded well with the value estimated from the PAP accumulation experiment shown in Fig. 6. This consistency in the values was unexpected because the steady-state method is principally different from the PAP accumulation technique, even though both can be carried out in the confined PDMS microwell system. For example at $t_{accu} = 31$ min, PAP accumulated within the microwell is estimated to be 8.8×10^{-14} mol, which corresponds to 12% of the initial amount of PAPG (7.26×10^{-13} mol) in the PDMS microwell whereas the PAP concentration is almost zero when the PAP oxidation current is in the steady state (150 s after the potential step to 0.3 V was applied).

Finally, the βGAL activity of yeast in the PDMS microwell was evaluated by the open-system method based on the spherical diffusion theory. In this method, the concentration profile of PAP was measured keeping the microwell uncovered. When a biologically active sample is localized at a spot on a solid support, the reactant and/or product forms a spherical concentration profile near the sample.[43,44] The mass transfer rate can be obtained by employing Fick's diffusion equation. Fig. 7 shows the oxidation current profile at the central axis of the well as a function of the height (z) from the top surface of the PDMS well entrapping 86 yeast cells. The tip scan rate and tip potential were set at 9.8 μm s^{-1} and +0.3 V, respectively. The tip current was converted to the PAP concentration using a calibration curve ($[C_{PAP}/mM] = 1.558 \times 10^{-1} \times [I/nA]$ for Fig. 7). The process for estimating the mass transfer rate from the spherical concentration profile has been described elsewhere.[43] The mass transfer rate for PAP production in the open system was estimated to be 4.91×10^{-18} mol s^{-1} $cell^{-1}$ by using the diffusion coefficient of PAP, 7.1×10^{-6} cm^2 s^{-1}.[45] For comparison, the PAP accumulation experiments were also performed using the same microwell accommodating 86 yeast cells, and the PAP production rate in this case was found to be 3.73×10^{-19} mol s^{-1} $cell^{-1}$ at $t_{accu} = 11$ min, which corresponded to only 7.6% of the βGAL activity obtained in the open system. By comparing the two experimental systems for several PDMS microwells accommodating 39–144 yeast cells ($n = 6$), we found that the βGAL activity in the confined PDMS microwell system is 4.3–16.3% of that in the open system. These results claim that the cellular enzymatic and metabolic activities may be strongly affected by the microenvironmental conditions, including the size and shape of the microwell and the density of the cellular sample in the microwell. In the case of the open system, the substrate, PAPG, could be supplied very quickly. However, as the PAPG is present in excess (7.4 mM) even in the confined PDMS microwell system, the supply rate does not cause any significant difference in the PAP production activity. Quinone imine (QI), the product of the electro-oxidation of PAP, has a relatively higher chemical activity than PAPG or PAP; further, it does not diffuse in the confined PDMS microwell system. However, in the open system

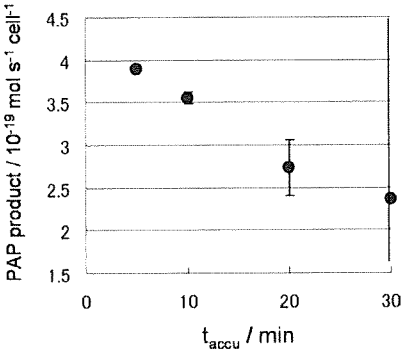

Fig. 6 Enzymatic activity (PAP production rate per cell) as a function of t_{accu}.

This journal is © The Royal Society of Chemistry 2009

shown in Fig. 7, QI produced at the scanning tip could be easily diluted. As shown in Fig. 4, the βGAL activity does not change and shows a good reproducibility when the same experiment is performed for three times, even at t_{accu} = 31 min; therefore, the βGAL inhibition by QI might not be irreversible.

4. Conclusions

A confined small volume was formed using a PDMS microwell array and a cap microelectrode with a relatively large seal radius. In the cyclic voltammetric measurements, the ferrocyanide ion entrapped in the microwell was oxidized with 100% efficiency, suggesting that a reproducible and quantitative electrochemical analysis was possible using this device. We also succeeded in evaluating the βGAL activity of recombinant yeast cells in the confined PDMS microwell. βGAL catalyzes the hydrolysis of PAPG to produce PAP, which is accumulated in the microwell. The accumulated PAP was quantitatively detected by amperometry using the abovementioned device. We have evaluated the βGAL activity by three different methods: the accumulation method, steady-state method, and open-system method. The βGAL activity estimated by the accumulation method was in good agreement with that estimated by the steady-state method. However, these βGAL activities estimated in the confined PDMS microwell were found to be considerably smaller than those estimated by the open-system method based on the spherical diffusion theory. This remarkable difference in the activities is probably because the concentrations of QI near the yeast cells are expected to be smaller for the open PDMS microwell than for the confined PDMS microwell. From the results obtained in the present work, we conclude that the cellular metabolic and enzymatic activities are considerably affected by the environmental conditions near the sample cells.

Acknowledgements

This work was partly supported by Grants-in-Aid for Scientific Research (18101006 and 19750055) from the Ministry of Education, Culture, Sports, Science and Technology (MEXT) and by the R & D Project for Environmental Nanotechnology from the Ministry of Environment.

References

1 C. Yi, C.-W. Li, S. Ji and M. Yang, *Anal. Chim. Acta*, 2006, **560**, 1–23.
2 C. N. LaFratta and D. R. Walt, *Chem. Rev.*, 2008, **108**, 614–637.
3 P. S. Dittrich and A. Manz, *Nat. Rev. Drug Discovery*, 2006, **5**, 210–218.
4 S. Yamamura, H. Kishi, Y. Tokimitsu, S. Kondo, R. Honda, S. R. Rao, M. Omori, E. Tamiya and A. Muraguchi, *Anal. Chem.*, 2005, **77**, 8050–8056.
5 I. Biran and D. R. Walt, *Anal. Chem.*, 2002, **74**, 3046–3054.
6 R. D. Whitaker and D. R. Walt, *Anal. Biochem.*, 2007, **360**, 63–74.
7 Y. Rondelez, G. Tresset, K. V. Tabata, H. Arata, H. Fujita, S. Takeuchi and H. Noji, *Nat. Biotechnol.*, 2005, **23**, 361–365.
8 L. Cai, N. Friedman and X. S. Xie, *Nature*, 2006, **440**, 358–362.
9 A. Groisman, C. Lobo, H. Cho, J. K. Campbell, Y. S. Dufour, A. M. Stevens and A. Levchenko, *Nat. Methods*, 2005, **2**, 685–649.
10 F. K. Balagadde, L. You, C. L. Hansen, F. H. Arnold and S. R. Quake, *Science*, 2005, **309**, 137–140.
11 W. DiLuzio, L. Turner, M. Mayer, P. Garstecki, D. B. Weibel, H. C. Berg and G. M. Whitesides, *Nature*, 2005, **435**, 1271–1274.
12 T. Saito, C.-C. Wu, H. Shiku, T. Yasukawa, M. Yokoo, T. Ito-Sasaki, H. Abe and T. Matsue, *Analyst*, 2006, **131**, 1006–1011.
13 Z. Lin, Y. Takahashi, Y. Kitagawa, T. Umemura, H. Shiku and T. Matsue, *Anal. Chem.*, 2008, **80**, 6830–6833.
14 W. Cheng, N. Klauke, H. Sedgwick, G. L. Smith and J. M. Cooper, *Lab Chip*, 2006, **6**, 1424–1431.
15 X. Cai, N. Klauke, A. Glidle, P. Cobbold, G. L. Smith and J. M. Cooper, *Anal. Chem.*, 2002, **74**, 908–914.
16 C. D. T. Bratten, P. H. Cobbold and J. M. Cooper, *Anal. Chem.*, 1998, **70**, 1164–117.
17 Z. P. Aguilar, W. R. Vandaveer and I. Fritsch, *Anal. Chem.*, 2002, **74**, 3321–3329.
18 J. C. Ball, D. L. Scott, S. Daunert, J. Wang and L. G. Bachas, *Anal. Chem.*, 2000, **72**, 497–501.
19 K. Nakatani, M. Sudo and N. Kitamura, *J. Phys. Chem. B*, 1998, **102**, 2908–2913.
20 N. Gao, X. Wang, L. Li, X. Zhang and W. Jin, *Analyst*, 2007, **132**, 1139–1146.
21 T. Yasukawa, A. Glidle, J. M. Cooper and T. Matuse, *Anal. Chem.*, 2002, **74**, 5001–5008.
22 R. Kashyap and M. Gratzl, *Anal. Chem.*, 1998, **70**, 1468–1476.
23 R. A. Clark, P. B. Hietpas and A. G. Ewing, *Anal. Chem.*, 1997, **69**, 259–263.
24 G. Wittstock, M. Burchardt, S. E. Pust, Y. Shen and C. Zhao, *Angew. Chem., Int. Ed.*, 2007, **46**, 1584–1617.
25 A. Schulte and W. Schuhmann, *Angew. Chem., Int. Ed.*, 2007, **46**, 8760–8777.
26 P. Sun and M. V. Mirkin, *Anal. Chem.*, 2007, **79**, 5809–5816.
27 F.-R. F. Fan, J. Kwak and A. J. Bard, *J. Am. Chem. Soc.*, 1996, **118**, 9669–9675.
28 M. V. Mirkin, L. O. Bulhoes and A. J. Bard, *J. Am. Chem. Soc.*, 1993, **115**, 201–204.
29 T. Yasukawa, K. Nagamine, Y. Horiguchi, H. Shiku, M. Koide, T. Itayama, F. Shiraishi and T. Matsue, *Anal. Chem.*, 2008, **80**, 3722–3727.
30 M. Badihi-Mossberg, V. Buchner and J. Rishpon, *Electroanalysis*, 2007, **19**, 2015–2028.
31 A. Schwartz-Mittelman, A. Baruch, T. Neufeld, V. Buchner and J. Rishpon, *Bioelectrochemistry*, 2005, **65**, 149–156.
32 A. Schwartz-Mittelman, T. Neufeld, D. Biran and J. Rishpon, *Anal. Biochem.*, 2003, **317**, 34–39.
33 J. Nishikawa, K. Saito, J. Goto, F. Dakeyama, M. Matsueo and T. Nishihara, *Toxcol. Appl. Pharmacol.*, 1999, **154**, 76–83.
34 F. Shiraishi, H. Shiraishi, J. Nishikawa, T. Nishihara and M. Morita, *J. Environ. Chem.*, 2000, **10**, 57–64.
35 S. Arulmozhiraja, F. Shiraishi, T. Okumura, M. Iida, H. Takigami, J. S. Edmonds and M. Morite, *Toxicol. Sci.*, 2005, **84**, 49–62.
36 C. K. Chow and S. P. Palecek, *Biotechnol. Prog.*, 2004, **20**, 449–456.
37 I. Biran, L. Kilmenty, R. H. Aronis, E. Z. Ron and J. Rishpon, *Microbiology*, 1999, **145**, 2129–2133.
38 T. Kaya, K. Nagamine, N. Matsui, T. Yasukawa, H. Shiku and T. Matsue, *Chem. Commun.*, 2004, 248–249.
39 K. Nagamine, S. Onodera, A. Kurihara, T. Yasukawa, H. Shiku, R. Asano, I. Kumagai and T. Matsue, *Biotechnol. Bioeng.*, 2007, **96**, 1008–1013.
40 C. Zhao, J. K. Sinha, C. A. Wijayawardhana and G. Wittstock, *J. Electroanal. Chem.*, 2004, **561**, 83–91.
41 N. Matsui, T. Kaya, K. Nagamine, T. Yasukawa, H. Shiku and T. Matsue, *Biosens. Bioelectron.*, 2006, **21**, 1202–1209.
42 H. Shiku, T. Saito, C.-C. Wu, T. Yasukawa, M. Yokoo, H. Abe, T. Matsue and H. Yamada, *Chem. Lett.*, 2006, **35**, 234–235.
43 T. Kaya, D. Numai, K. Nagamine, S. Aoyagi, H. Shiku and T. Matsue, *Analyst*, 2004, **129**, 529–534.
44 H. Shiku, T. Shiraishi, S. Aoyagi, Y. Utsumi, M. Matsudaira, H. Abe, H. Hoshi, S. Kasai, H. Ohya and T. Matsue, *Anal. Chim. Acta*, 2004, **522**, 51–58.
45 O. Niwa, Y. Xu, H. B. Halsall and W. R. Heineman, *Anal. Chem.*, 1993, **65**, 1559–1563.

Analytica Chimica Acta 640 (2009) 87–92

Contents lists available at ScienceDirect

Analytica Chimica Acta

journal homepage: www.elsevier.com/locate/aca

Development of electrochemical reporter assay using HeLa cells transfected with vector plasmids encoding various responsive elements

Hitoshi Shiku [a,*], Michiaki Takeda [a], Tatsuya Murata [a], Uichi Akiba [b], Fumio Hamada [b], Tomokazu Matsue [a,**]

[a] Graduate School of Environmental Studies, Tohoku University, 6-6-11-604 Aramaki-Aoba, Sendai 980-8579, Japan
[b] Graduate School of Engineering & Resource Science, Akita University, 1-1 Tegata gakuen-machi, Akita 010-8502, Japan

ARTICLE INFO

Article history:
Received 27 December 2008
Received in revised form 11 March 2009
Accepted 12 March 2009
Available online 20 March 2009

Keywords:
Reporter assay
Scanning electrochemical microscopy
Chemiluminescence
Responsive element
Signal transduction
Alkaline phosphatase

ABSTRACT

Electrochemical assay using HeLa cell lines transfected with various plasmid vectors encoding SEAP (secreted alkaline phosphatase) as the reporter has been performed by using SECM (scanning electrochemical microscopy). The plasmid vector contains different responsive elements that include GRE (glucocorticoid response elements), CRE (cAMP responsive elements), or κB (binding site for NFκB (nuclear factor kappa B)) upstream of the SEAP sequence. The transfected HeLa cells were patterned on a culture dish in a 4 × 4 array of circles of diameter 300 μm by using the PDMS (poly(dimethylsiloxane)) stencil technique. The cellular array was first exposed to 100 ng mL^{-1} dexamethasone, 10 ng mL^{-1} forskolin, or 100 ng mL^{-1} TNF-α (tumor necrosis factor α) after which it was further cultured in an RPMI culture medium for 6 h. After incubation, the cellular array was soaked in a measuring solution containing 4.7 mM PAPP (p-aminophenylphosphate) at pH 9.5, following which electrochemical measurements were performed immediately within 40 min. The SECM method allows parallel evaluation of different cell lines transfected with pGRE-SEAP, pCRE-SEAP, and pNFκB-SEAP patterned on the same solid support for detection of the oxidation current of PAP (p-aminophenol) flux produced from only 300 HeLa cells in each stencil pattern. The results of the SECM method were highly sensitive as compared to those obtained from the conventional CL (chemiluminescence) protocol with at least 5 × 10^4 cells per well.

© 2009 Elsevier B.V. All rights reserved.

1. Introduction

Whole-cell biosensors refer to electrochemical and/or optical biosensors that utilizes "whole cells" instead of purified enzymes for converting specific chemical inputs into signals. Gene engineering has been evolutionally expanded the field of the cell-based biosensor because the genetically modified cell itself functions as a transducer to produce a measurable signal, reporter protein such as green fluorescence protein, chloramphenicol acetyl transferase, luciferase, beta-galactosidase, or secreted alkaline phosphatase (SEAP). These proteins are generated in response to various analytes that possibly activate/suppress gene expressions at a transcriptional level [1,2]. The reporter assay is frequently used by introducing a vector plasmid containing the sensing element upstream of a reporter gene. Sensitive and selective detection of metals, hydrocarbons, mutagens, and pollutants can be achieved by the use of genetically engineered whole-cell biosensors [1]. More importantly, the whole-cell reporter assay allows the evaluation of signal pathways that are activated, namely the intracellular mechanisms of action against specific drugs and toxins [3–5]. Expression vectors, which contain reporter genes controlled by a specific transcription factor consensus sequence, are used to study transcription factors and cellular signaling mechanisms. In fact, there are several commercially available kits that can determine the involvement of various response element-binding proteins in signal transduction pathways. Parallel evaluation of signaling pathways can be accomplished by combining cellular array technology with cells transfected with different types of plasmid vectors [6].

Recent advances in microfluidics and sensor miniaturization have resulted in rapid, cheap, and integrated analysis using closed microfluidic systems [7–9]. Cellular array chips play a significant role in realizing a high-throughput screening, especially in a manner similar to reverse transfection [10–12]. Gene introduction on cellular chips is not always helpful because of increase in the heterogeneity of the cellular status, low reliability, and a long assay time. We have developed various types of cellular chips on which cell culture [13–16], differentiation [17–19], manipulation [20–22], stimulation [23], gene introduction [24], and controlling of cellular polarity processes [25] were electrochemically detected. In many cases chemical stimulation of cells for gene expression was carried

* Corresponding author. Tel.: +81 22 795 6167; fax: +81 22 795 6167.
** Corresponding author.
E-mail addresses: shiku@bioinfo.che.tohoku.ac.jp (H. Shiku), matsue@bioinfo.che.tohoku.ac.jp (T. Matsue).

0003-2670/$ – see front matter © 2009 Elsevier B.V. All rights reserved.
doi:10.1016/j.aca.2009.03.018

out in the pre-culture stage before immobilizing the cells on the chip, since it could not be accomplished on a chip [17,18,21,22,26].

In the present study, cells transfected with different plasmid constructs were cultured as monolayers on a stencil-masked solid support [27–30]. Cellular signal transduction is triggered with the help of chemical stimulation performed on a solid support. To obtain parallel responses from each of the cell lines with a certain number of cells (300 cells arranged in a circular pattern with a diameter of 300 μm), the stencil sheet was peeled off just before the electrochemical measurement to form the cellular pattern. The expression of SEAP was electrochemically evaluated after stimulating each signal transduction pathway with the triggering chemicals. The cellular status in the monolayer culture system used in the present study was also evaluated for the stencil-based culture in the medium after exchanging it with the measuring solution (pH 9.5).

2. Experimental

2.1. Materials

p-Aminophenol (PAP, Wako Pure Chemical Industries), dexamethasone (Wako Pure Chemical Industries), forskolin (Sigma), tumor necrosis factor α (TNF-α, Wako Pure Chemical Industries), 2-[4-(2-hydroxyethyl)-1-piperazinyl] ethanesulfonic acid (HEPES, Dojindo Laboratories, Japan), 3,3,4,4,5,5,6,6,6,-nonafluorohexyltrichlorosilane (LS-912, Shin-etsu Chemical Co. Ltd.), RPMI-1640 (Gibco Invitrogen, Tokyo, Japan), fetal bovine serum (FBS, Gibco), collagen type I-A (Nitta Gelatin, Japan), penicillin (Gibco), streptomycin (Gibco), Mercury™ pathway profiling system (BD Sciences), Opti-MEM I medium (Gibco), LipofectAMINE 2000 (Invitrogen), poly(dimethylsiloxane) (PDMS, Silpot 184W/C, Dow Corning, USA), and others chemicals were used as received. The Mercury™ pathway profiling system is a set of expression vector sets that contain a distinct enhancer element upstream of a reporter gene—SEAP. Various intracellular signal transduction pathways were assessed by employing these vector sets with their corresponding enhancer elements—GRE (glucocorticoid response elements), CRE (cAMP response element), κB (kappa B), AP1 (activator protein 1), HSE (heat shock element), NFAT (nuclear factor of activated T cells), Myc (E-box DNA binding protein), and SRE (serum-response element). Three of the eight reporter genes showed activity above baseline after a 24-h stimulation—GRE, CRE, and NFκB. The responsive elements GRE, CRE, and κB are specific DNA sequences called enhancers to which the transcription factors GREB (GRE binding protein), CREB (CRE binding protein), and NFκB (nuclear factor κB) bind. The pSEAP2 series is an integrated set of plasmids that differs only with regard to the presence or absence of the simian virus 40 (SV40) promoter and/or enhancer sequence. The pSEAP2-Control vector contains the SEAP structural gene that is under the transcriptional control of the SV40 promoter and enhancer, whereas the pSEAP2-basic vector contains the SEAP gene without promoter/enhancer. p-Aminophenylphosphate (PAPP) monosodium salt was purchased from LKT Lab Inc. or synthesized according to the procedure described in the literature [31,32].

2.2. Cell culture and transfection

HeLa cells were donated by the Cell Resource Center for Biomedical Research (Tohoku University). The cells were cultured in RPMI-1640 containing 10% FBS, 50 μg mL^{-1} penicillin, and 50 μg mL^{-1} streptomycin at 37 °C in a humidified atmosphere containing 5% CO_2. HeLa cells were transfected with the expression vector set of Mercury™ Pathway Profiling System. The cells were seeded in a 35-mm dish (Falcon) at a density of 5×10^5 cells in 2 mL of RPMI-1640 medium containing 10% FBS without antibiotics. A day after the cultivation, transfection was performed by the addition of 500 μL of Opti-MEM I medium containing 4 μg of plasmid DNA and 10 μL of LipofectAMINE 2000; then, incubation was carried out for 5 h. Subsequently, the transfection medium changed to a pure culture medium, and the cells were incubated at 37 °C overnight.

2.3. Electrochemical assay of cellular array patterned using a PDMS stencil technique

The transfected HeLa cells were patterned on a culture dish in an array of circles of diameter 300 μm by using a PDMS stencil. A PDMS stencil sheet of a thickness of 100 μm was prepared from a PDMS-curing agent mixture (10:1, w/w), and the thickness of the PDMS sheet was controlled by a spin coater (1000 rpm, 30 s). The fabrication procedure is described elsewhere [33,34]. In the PDMS stencil, the 4×4 hole-array of diameter 300 μm was drawn using a CO_2 laser engraving system (Universal Laser System Inc.) and treated with an O_2 plasma (plasma asher LTA-101, Yanaco, 100 W, 13.6 MHz, 15 s, O_2 flow rate: 40 mL min^{-1}). The PDMS stencil sheet was soaked into a 70% ethanol solution for 30 min and placed at the bottom of the culture dish of diameter 35 mm; the sheet was then placed on a clean bench and irradiated with a UV lamp for 30 min. The HeLa cells were suspended in a medium to achieve a final concentration of 1.5×10^6 cells mL^{-1}; 150 μL of this suspension was seeded into the PDMS stencil. The stencil was then incubated for 4 h at 37 °C in a humidified atmosphere containing 5% CO_2. Two milliliters of the medium, which included the stimulation chemical reagent (final concentrations: 100 ng mL^{-1} dexamethasone, 10 μg mL^{-1} forskolin, or 100 ng mL^{-1} TNF-α), was added and further incubated for 6–24 h at 37 °C in a humidified atmosphere containing 5% CO_2. Stock solutions of dexamethasone and forskolin were diluted with dimethyl sulfoxide (DMSO, Wako Pure Chemical Industries) and stored at −20 °C. Dexamethasone, forskolin, and TNF-α were selected as the characteristic stimuli for the signaling pathways of GRE, PKC (protein kinase C)/CREB, and NFκB, respectively.

The scanning electrochemical microscope consisted of a Pt microdisk (diameter: 20 μm) as the working electrode and a Ag/AgCl reference/counter electrode [3,35]. The electrode potential was set at 0.3 V vs Ag/AgCl for facilitating the oxidation of PAP. For the SECM measurements, the PDMS stencil sheet was peeled off and the culture dish was immediately washed twice with HEPES buffer and was placed into 2 mL of the measuring solution containing 4.7 mM PAPP and HEPES buffer (pH 9.5). The electrochemical measurements were completed within 5 min for each line scan of 1500 μm at a rate of 50 μm s^{-1} at room temperature. Normally, SECM imaging with a resolution of 1000 μm × 1000 μm takes approximately 30 min (20 lines at 20 μm s^{-1}). The tip-scanning height from the substrate surface was set at 50 μm. Viability of the cells patterned on the stencil, under the conditions used during SECM measurements was evaluated by a live/dead fluorescence kit (a combination of two fluorochromes, calcein-AM and propidium iodide, Dojindo Laboratories, Japan). The results of the evaluation indicated that almost all the cells were alive for a period of 60 min after they were soaked in the measuring solution (pH 9.5). For static analysis, the SECM measurement was repeated for more than six times ($n \geq 6$) in order to compare the current responses with and without stimulation for each of the transfected HeLa cell lines.

2.4. Chemiluminescence (CL) SEAP assay

The SEAP activity was evaluated using a Great EscAPe™ SEAP chemiluminescence detection kit (BD Sciences) in accordance with the recommended protocol [3]. Briefly, the transfected HeLa cells were seeded in collagen-coated 96-well plates (Cellmatrix Type I-C, Nitta Gelatin) at a rate of 5×10^5 cells per well and were incubated for 4 h. After observation of cell adhesion, a stimulus solution was added, and the cells were further incubated for 24 h. Fifteen microliters of the culture medium was sampled from each well for the CL SEAP assay. The sampled culture medium was mixed with 45 μL of dilution buffer and incubated at 65 °C for 30 min in order to inhibit endogenous phosphatase activity. Since the reporter proteins SEAP and SEAP2 were heat protective, only the expressing SEAP activity could be measured after the heat shock. The sample was first mixed with 60 μL of the assay buffer (pH 10.3) for 5 min at room temperature and then with 60 μL of the chemiluminescence solution containing 1.25 mM CSPD (disodium 3-(4-methoxyspiro [1,2-dioxetane-3,2′-(5′-chloro)-tricyclo [3,3,1,1^{3,7}]decan]-4-yl)phenyl phosphate). After incubating the sample in the dark for 10 min, the CL signals were detected using a high-performance intensified CCD camera (PI-MAX 512RB, Princeton Instruments) [3,19]. The assays were repeated thrice under each experimental condition ($n = 3$).

3. Results and discussion

Fig. 1a shows the CL intensities of 5×10^4 cells of non-transfected HeLa (wild type) cells and HeLa cells transfected with the SEAP plasmids of negative (pSEAP2-Basic) and positive controls (pSEAP2-Control) according to the conventional 96-well based assay. In the CL assay protocol, 15 μL of the culture medium was required for sampling, and the sample was further treated at 65 °C for 30 min in order to deactivate the background activities of alkaline phosphatase. Fig. 1b shows the CL results obtained for the HeLa cells transfected with pGRE-SEAP, pCRE-SEAP, or pNFκB-SEAP 24 h after stimulation. Dexamethasone [6,36,37], forskolin [38], or TNF-α [6,39] was chosen as the stimulus and was compared with the cases without stimulation. As a negative control, the alkaline phosphatase activities of the HeLa cells transfected with pSEAP-Basic were also evaluated under each stimulation condition. The CL responses to stimulus exposure were precisely observed for all the transfected HeLa cell lines. The evaluated concentration ranges for the stimuli were 10–10^4 ng mL^{-1} for dexamethasone, 10–10^3 μg mL^{-1} for forskolin, and 10–100 ng mL^{-1} for TNF-α. The linearity of the calibration plot between the CL response and the stimulus concentration was poor. It was also difficult to increase the linearity of the response by increasing the concentration of the stimulus in the electrochemical assay. The values of the signal to noise ratio (S/N), which is defined as the intensity for adding stimulus normal

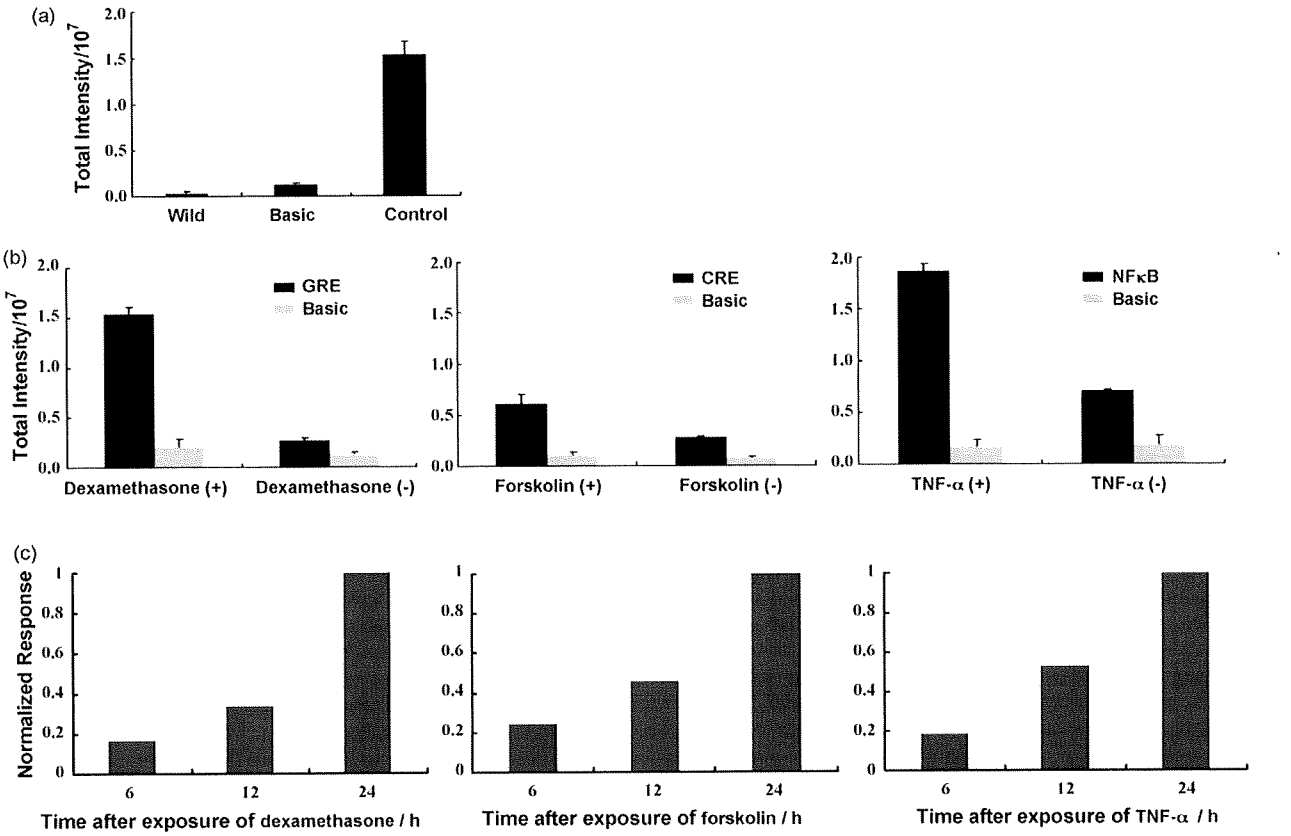

Fig. 1. (a) SEAP activity based on the CL assay for the wild-type HeLa cells and HeLa cells transfected with pSEAP2-Basic (negative control) and pSEAP2-Control (positive control). (b) CL SEAP assay for HeLa cells transfected with pGRE-SEAP, pCRE-SEAP, and pNFκB-SEAP. Dexamethasone (100 ng mL^{-1}), forskolin (10 μg mL^{-1}), and TNF-α (100 ng mL^{-1}) were added as stimuli and the results obtained were compared with those without the stimulus. (c) CL SEAP assay as a function of time after the addition of the stimulus (dexamethasone, forskolin, or TNF-α). Control indicates HeLa cells transfected with pSEAP2-Control (positive control) without the stimuli.

to that without stimulation, were 5.8, 2.2, and 2.6 for dexamethasone, forskolin, and TNF-α, respectively. In the case of the NFκB pathway stimulated with TNF-α, the signal (result obtained with stimulation) as well as the noise level (result obtained without stimulation) was the highest among the three experiments. Fig. 1c shows the CL intensities as a function of time after stimulation for HeLa cells transfected with pGRE-SEAP, pCRE-SEAP, and pNFκB-SEAP. Dexamethasone (100 ng mL^{-1}), forskolin (10 μg mL^{-1}), and

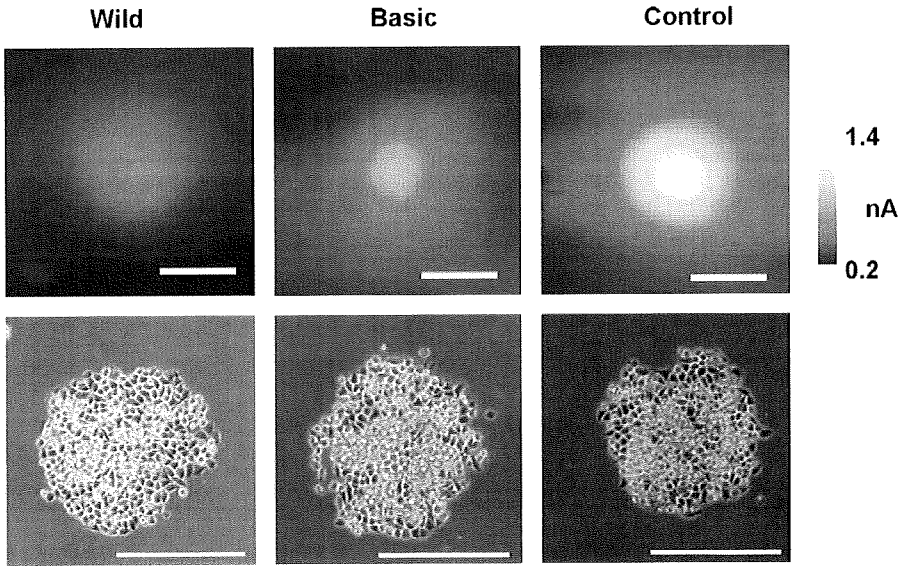

Fig. 2. SECM images of the stencil-patterned HeLa cells (~300 cells) transfected with pSEAP2-Control (positive control), pSEAP2-Basic (negative control), and the wild-type HeLa cells. A Pt disk with a diameter of 20 μm was used as the probe electrode. Optical micrographs for the corresponding HeLa cells are also shown. Bar: 300 μm.

TNF-α (100 ng mL^{-1}) were added as stimuli in the microtiter plate and incubated for 6, 12, and 24 h, respectively. HeLa cells (pSEAP2-Control) were suspended in the culture medium and incubated and used as the positive control. Since the secreted alkaline phosphatase accumulated in the medium in the microtiter plate well, the chemical intensities of all the four transfected HeLa cell lines increased linearly with the exposure time.

Fig. 2 shows the SECM images along with the corresponding optical microscope images for non-transfected HeLa cells (wild type) and HeLa cells transfected with SEAP plasmids of negative (pSEAP2-Basic) and positive controls (pSEAP2-Control) that were patterned using a PDMS stencil of diameter 300 μm. The number of cells in the patterns, which was counted manually, was found to be about 300. SEAP was secreted from the patterned cells into the surrounding medium and then the enzymatic substrate PAPP was hydrolyzed to PAP, which was electrochemically oxidized at the probe electrode. The oxidation current of 1.35 ± 0.417 nA (n = 7) for HeLa transfected with pSEAP2-Control was obtained with the substrate generation/tip collection mode SECM. It was found from a calibration curve that the oxidation current value corresponds to a local PAP concentration of ~0.45 mM, which is considerably smaller than the bulk PAPP concentration (4.7 mM). The oxidation current profiles were almost stable during the time-scale of SECM imaging (about 30 min per image) that suggested the concentration profile of PAP near the circle cellular pattern were in steady state. The PAP concentration profile was in accordance with a hemispherical diffusion theory and not disturbed by the diffusion of SEAP enzyme. Background currents for the wild-type HeLa cells and HeLa cells transfected with pSEAP2-Basic were 0.622 ± 0.042 (n = 4) and 0.731 ± 0.208 nA (n = 3), respectively. Since the levels of background currents for the two cell lines were almost similar, it could be concluded that these currents were due to the original (endogeneous) activity of alkaline phosphatase present in the HeLa cells and not due to SEAP secreted from pSEAP2-Basic.

The SECM assay is advantageous to detect the localized flux for the product (PAP) of the enzymatic reaction [26] with a probe microelectrode and a relatively small number of cells (~300) is enough to monitor the PAP concentration profile near the cellular sample. The volume of the measuring solution (2 mL) must be sufficiently large compared to the local enzymatic reaction rate, otherwise the concentration of both SEAP and PAP in bulk solution would elevate and the oxidation current profile becomes broader. On the contrary, the CL assay was performed with conventional 96-well plates. The SEAP activity within the solution of the total 180 μL was detected with a high-performance intensified CCD camera. At least 10^4 cells were required to detect CL signal in our system.

Table 1
SECM response [(average ± standard deviation)/nA] (n = sample number) for various stimulus reagents corresponding to the plasmids transfected into the HeLa cells.

	Stimulus		
	Dexamethasone	Forskolin	TNF-α
Plasmid	pGRE	pCRE	pNFκB
(+)	1.09 ± 0.175 (8)	1.46 ± 0.192 (17)	1.38 ± 0.312 (6)
(−)	0.632 ± 0.120 (8)	1.18 ± 0.102 (14)	0.861 ± 0.139 (7)
p	<0.005	<0.001	<0.005
S/N	1.73	1.23	1.60

The selection of the cell type is important to obtain sufficient reporter signals. HepG2 (human hapatoma cell line) [6], HEK293 (human embryonic kidney) [10], MCF-7 (human breast cancer cell line) [3], and HeLa cell lines were transfected with pSEAP2-Control vector and it was found that HeLa cells showed the highest gene expression activity. In the case that a MCF-7 was selected and transfected with pSEAP2-Control, the PAP oxidation current for the stencil-patterned cells was 2.0 pA with an SECM assay (data not shown). The CL evaluations demonstrated that the SEAP activity of the transfected HeLa cells was at least 4-fold larger than that of the transfected MCF-7. However, the background response for HeLa cells transfected with pSEAP2-Basic increased considerably, whereas that for MCF-7 cells transfected with pSEAP2-Basic was almost negligible.

Next the one-line SECM scans for the HeLa cells transfected with pGRE-SEAP, pCRE-SEAP, and pNFκB-SEAP were evaluated

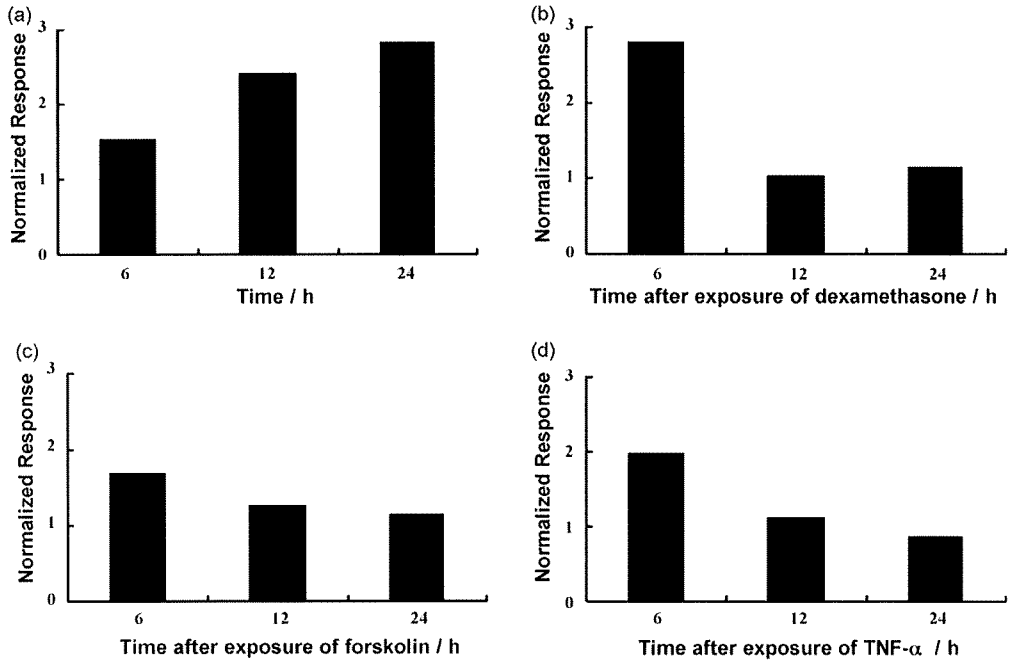

Fig. 3. SECM assay as a function of time after the addition of the stimulus (dexamethasone (b), forskolin (c), or TNF-α (d)) for the stencil-patterned HeLa cells transfected with pGRE-SEAP (b), pCRE-SEAP (c), and pNFκB-SEAP (d), respectively. Control indicates the HeLa transfected with pSEAP2-Control (positive control) without stimulus reagent (a).

with (+) and without (−) dexamethazone (100 ng mL^{-1}), forskolin (10 μg mL^{-1}), and TNF-α (100 ng mL^{-1}), respectively. Table 1 shows the summarized SECM responses for various stimulations. The response obtained 6 h after the stimulation was compared with that without the stimulation. The current response in the SECM assay is determined by subtracting the background response (the current at a distance of 600 μm from the center of the circular pattern of the HeLa cells) from current at the center. The maximum response was observed for CRE (1.46 ± 0.192 nA (n = 17)), the minimum for GRE (1.09 ± 0.175 nA (n = 8)), and an intermediate response for NFκB (1.38 ± 0.312 nA (n = 6)). The response was normalized to the corresponding result without stimulation and defined as signal to noise ratio (S/N) because the SECM response tended to vary with the cellular status of the cultured host and the transfection conditions. Typically, the current response without stimulation ranged from 0.12 to 0.6 nA, during the experiments have been performed for 1 year. The responses obtained were in the following order: GRE (S/N = 1.73) > NFκB (S/N = 1.60) > CRE (S/N = 1.23). Since the S/N ratios obtained were different from one another, all the three responses with and without the stimuli were found to be statistically distinguishable (t-test, $p < 0.005$).

Fig. 3 shows time dependency after stimulation. The SECM responses were normalized to those without stimulation. HeLa cells transfected with pSEAP2-Control were also evaluated in the medium under conditions identical to those used in the SECM measurements and normalized to the response for the HeLa transfected with pSEAP2-Basic (Fig. 3a). Among the responses (Fig. 3b–d) obtained for the three signal pathways evaluated 6 h, 12 h, and 24 h after the stimulation, the response 6 h after the stimulation was the maximum. This type of signal degradation during longer timescale incubation has also been observed in the other reporter assay systems, especially those based on electrochemical cellular chips utilizing bacteria and mammalian cells [3,17]. On the contrary, the current responses for the positive control 12 h and 24 h after incubation were almost identical to or slightly larger than those 6 h after the incubation. This result suggests that the cells patterned using the stencil technique facilitates the maintenance of cellular functions during a 24-h incubation.

Arraying cell lines transfected with different plasmids on a solid support may be the most suitable electrochemical reporter assay for the evaluation of various signaling pathways. Fig. 4a shows the responses to the one-line SECM scans for HeLa cells transfected with pGRE-SEAP, pCRE-SEAP, and pNFκB-SEAP patterned on the same culture dish 6 h after the addition of 100 ng mL^{-1} dexamethasone. The results obtained in the CL assay are also shown in Fig. 4b. Dexamethasone is known as a typical stimulus of GR pathway [36,37], and therefore, the current response is the highest for the cells transfected with pGRE-SEAP. Interestingly, the current signal for pCRE-SEAP is also significantly greater than that observed before the addition of dexamethasone. However, the signal for pNFκB-SEAP was not influenced by dexamethasone addition. The current responses obtained on a single solid support corresponded well with the CL results obtained at a level of ~10^4 cells. The responses to the one-line SECM scans for the cellular arrays of the three transfected HeLa cell lines 6 h after the addition of 10 μg mL^{-1} forskolin and 100 ng mL^{-1} TNF-α are shown in Fig. 4c and e, respectively. The

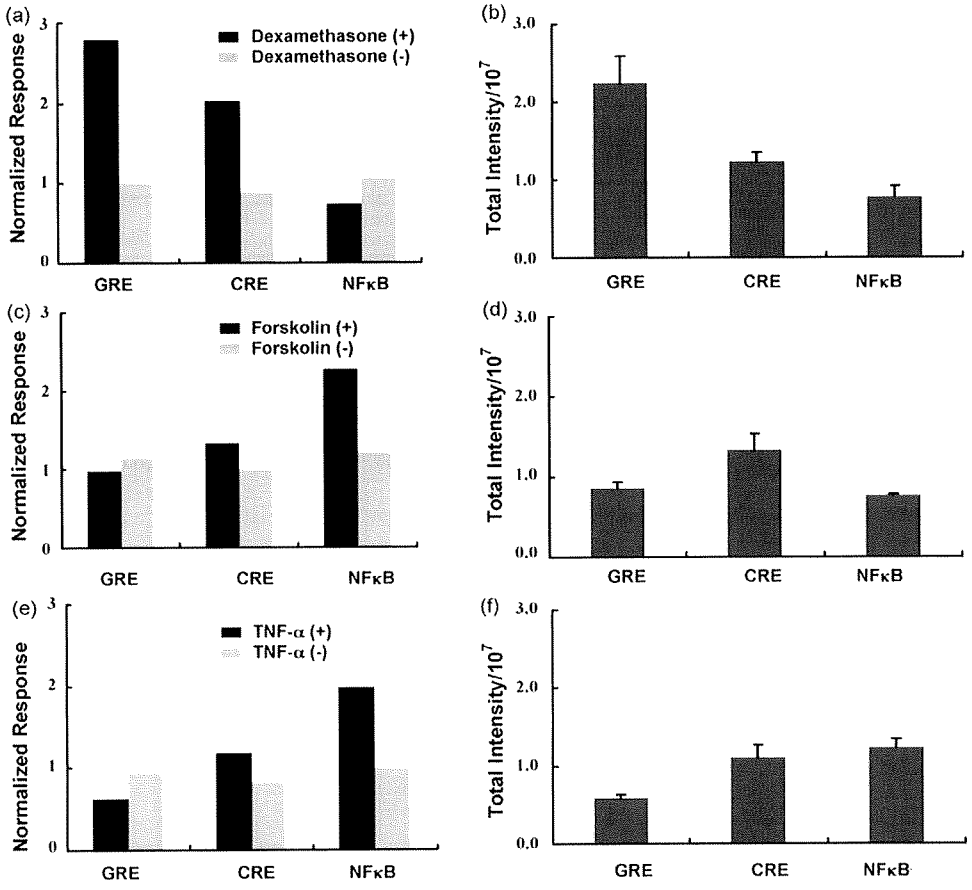

Fig. 4. SECM responses (a, c and e) of the stencil-patterned HeLa cells transfected with pGRE-SEAP, pCRE-SEAP, and pNFκB-SEAP. The results of the CL SEAP assay (b, d and f) are also shown. Dexamethasone (a and b, 100 ng mL^{-1}), forskolin (c and d, 10 μg mL^{-1}), and TNF-α (e and f, 100 ng mL^{-1}) were added as stimuli and incubated for 6 h for SECM and 24 h for CL.

results of the CL assays are shown in Fig. 4d and f. In all the cases, the electrochemical and CL results were in good agreement.

Overall, the electrochemical reporter assay may be suitable for qualitative screening but not very useful for quantitative evaluation of the calibration curves between the response and the ligand concentrations. Consequently, static analysis should be performed for each of the stimulation reagents in order to judge whether cellular signal transduction is activated or not. In the future, we plan to design an integrated electrochemical cellular device that allows a rapid and high-throughput analysis. However, as discussed in this study, SECM characterization before integration of the electrode array and the cellular chip is powerful and essential for the evaluation of certain cellular signal transduction pathways and cellular status patterned on the solid supports.

4. Conclusion

SECM was used for the preparation of an electrochemical reporter assay from HeLa cells transfected with plasmids coding various responsive elements. Genetically engineered HeLa cells were arrayed on a glass substrate with a PDMS stencil, and the cellular status of the stencil-patterned cell array was found to be normal for a 24-h incubation in a medium with various stimulus reagents as well as a 60-min exposure to the measuring solution of pH 9.5. The GRE, CRE, and NFκB signal pathways were all electrochemically monitored using the stencil-patterned HeLa cell arrays. The electrochemical responses were also compared with the results of the CL assay, which required a concentration of 5×10^4 cells per well. In contrast, the SECM assay can be performed with ~300 cells, and it neither requires medium sampling nor deactivation for inhibition of the endogenous phosphatase activity.

Acknowledgements

This work was partly supported by a Grant-in-Aid for Scientific Research on Priority Areas (17066002) "Life Surveyor" from the Ministry of Education, Culture, Sports, Science and Technology (MEXT) of Japan; by Grants-in-Aid for Scientific Research (18101006 and 19750055) from MEXT; and by a grant from the Center for Interdisciplinary Research, Tohoku University.

References

[1] S. Daunert, G. Barrett, J.S. Feliciano, R.S. Shetty, S. Shrestha, W.S. Spencer, Chem. Rev. 100 (2000) 2705–2738.
[2] T. Matsue, H. Shiku, Electrochemistry 74 (2006) 107–113.
[3] Y.S. Torisawa, N. Ohara, K. Nagamine, S. Kasai, T. Yasukawa, H. Shiku, T. Matsue, Anal. Chem. 78 (2006) 7625–7631.
[4] K.Y. Inoue, T. Yasukawa, H. Shiku, T. Matsue, Electrochemistry 76 (2008) 525–528.
[5] E. Kelso, J. McLean, M.F. Cardosi, Electroanalysis 12 (2000) 490–494.
[6] K.R. King, S. Wang, D. Irima, A. Jayaraman, M. Toner, M.L. Yarmush, Lab Chip 7 (2007) 77–85.
[7] C. Yi, C.-W. Li, S. Ji, M. Yang, Anal. Chim. Acta 560 (2006) 1–23.
[8] C.E. Sims, N.L. Allbritton, Lab Chip 7 (2007) 423–440.
[9] J. El-Ali,,P.K. Sorger, K.F. Jensen, Nature 442 (2006) 403–411.
[10] J. Ziauddin, D.M. Sabatini, Nature 411 (2001) 107–110.
[11] J.B. Delehanty, K.M. Shaffer, B. Lin, Biosens. Bioelectron. 20 (2004) 773–779.
[12] S. Fujita, E. Ota, C. Sakaki, K. Takano, M. Miyake, J. Miyake, J. Biotechnol. 104 (2007) 329–333.
[13] T. Kaya, K. Nagamine, D. Oyamatsu, H. Shiku, M. Nishizawa, T. Matsue, Lab Chip 3 (2003) 320–324.
[14] Y.S. Torisawa, T. Kaya, T. Takii, D. Oyamatsu, M. Nishizawa, T. Matsue, Anal. Chem. 73 (2003) 2154–2158.
[15] Y.S. Torisawa, A. Takagi, Y. Nashimoto, T. Yasukawa, H. Shiku, T. Matsue, Biomaterials 28 (2007) 559–566.
[16] H. Kimura, T. Yamamoto, H. Sakai, Y. Sakai, T. Fujii, Lab Chip 8 (2008) 741–746.
[17] T. Kaya, K. Nagamine, N. Matsui, T. Yasukawa, H. Shiku, T. Matsue, Chem. Commun. (2004) 248–249.
[18] K. Nagamine, N. Matsui, T. Kaya, T. Yasukawa, H. Shiku, T. Nakayama, T. Nishino, T. Matsue, Biosens. Bioelectron. 21 (2005) 145–151.
[19] S. Kasai, H. Shiku, Y.S. Torisawa, H. Noda, J. Yoshitake, T. Shiraishi, T. Yasukawa, T. Watanabe, T. Matsue, T. Yoshimura, Anal. Chim. Acta 549 (2005) 14–19.
[20] M. Suzuki, T. Yasukawa, H. Shiku, T. Matsue, Biosens. Bioelectron. 24 (2008) 1043–1047, doi:10.1016/j.bios.2008.06.051.
[21] T. Yasukawa, K. Nagamine, Y. Horiguchi, H. Shiku, M. Koide, T. Itayama, F. Shiraishi, T. Matsue, Anal. Chem. 80 (2008) 3722–3727.
[22] H. Shiku, S. Goto, S. Jung, K. Nagamine, M. Koide, T. Itayama, T. Yasukawa, T. Matsue, Analyst 134 (2009) 182–187.
[23] Y. Torisawa, H. Shiku, T. Yasukawa, M. Nishizawa, T. Matsue, Biomaterials 26 (2005) 2165–2172.
[24] K. Nagamine, S. Onodera, Y. Torisawa, T. Yasukawa, H. Shiku, T. Matsue, Anal. Chem. 77 (2005) 4278–4281.
[25] Y.S. Torisawa, Y. Nashimoro, T. Yasukawa, H. Shiku, T. Matsue, Biotechnol. Bioeng. 97 (2007) 615–621.
[26] N. Matsui, T. Kaya, K. Nagamine, T. Yasukawa, H. Shiku, T. Matsue, Biosens. Bioelectron. 21 (2006) 1202–1209.
[27] A. Folch, B.-H Jo, O. Hurtado, D.J. Beebe, M. Toner, J. Biomed. Mater. Res. 52 (2000) 346–353.
[28] A. Tourovskaia, T. Barber, B.T. Wickes, D. Hirdes, B. Grin, D.G. Castner, K.E. Healy, A. Folch, Langmuir 19 (2003) 4754–4764.
[29] D. Wright, B. Rajalingam, S. Selvarasah, M.R. Dokmeci, A. Khademhosseini, Lab Chip 7 (2007) 1272–1279.
[30] S. Jinno, H.-C. Moeller, C.-L. Chen, B. Rajalingam, B.G. Chung, M.R. Dokmeci, A. Khademhosseini, J. Biomed. Mater. Res. A 86 (2008) 278–288.
[31] L.H. DeRiemer, C.F. Meares, Biochemistry 20 (1981) 1606–1612.
[32] R.Q. Thompson, G.C. Barone III, H.B. Halsall, W.R. Heineman, Anal. Biochem. 192 (1991) 90–95.
[33] C.-C. Wu, T. Yasukawa, H. Shiku, T. Matsue, Sens. Actuators B 110 (2005) 342–349.
[34] Y. Takahashi, T. Miyamoto, H. Shiku, R. Asano, T. Yasukawa, I. Kumagai, T. Matsue, Anal. Chem. 81 (2009) 2785–2790.
[35] G. Wittstock, M. Burchardt, S.E. Pust, Y. Shen, C. Zhao, Angew. Chem. Int. Ed. 46 (2007) 1584–1617.
[36] A. Kelly, H. Bowen, Y.-K. Jee, N. Mahfiche, C. Soh, T. Lee, C. Hawrylowicz, P. Lavender, J. Allergy Clin. Immunol. 121 (2008) 203–208.
[37] T. Mori, F. Saito, T. Yoshino, H. Takeyama, T. Matsunaga, Biotechnol. Bioeng. 99 (2008) 1453–1461.
[38] R. Trevisan, L. Daprai, L. Paloschi, N. Vajente, L. Chieco-Bianchi, D. Saggioro, Exp. Cell Res. 312 (2006) 1390–1400.
[39] I. Tattoli, L.A. Carnerio, M. Jehanno, J.G. Magalhaes, Y. Shu, D.J. Philpott, D. Arnoult, S.E. Girardin, EMBO Rep. 9 (2008) 293–300.

analytical chemistry

Subscriber access provided by TOHOKU UNIV

Article

Electrochemical Detection of Epidermal Growth Factor Receptors on a Single Living Cell Surface by Scanning Electrochemical Microscopy

Yasufumi Takahashi, Takeshi Miyamoto, Hitoshi Shiku, Ryutaro Asano, Tomoyuki Yasukawa, Izumi Kumagai, and Tomokazu Matsue

Anal. Chem., **2009**, 81 (7), 2785-2790• DOI: 10.1021/ac900195m • Publication Date (Web): 05 March 2009

Downloaded from http://pubs.acs.org on April 6, 2009

More About This Article

Additional resources and features associated with this article are available within the HTML version:

- Supporting Information
- Access to high resolution figures
- Links to articles and content related to this article
- Copyright permission to reproduce figures and/or text from this article

View the Full Text HTML

ACS Publications
High quality. High impact.

Analytical Chemistry is published by the American Chemical Society. 1155 Sixteenth Street N.W., Washington, DC 20036

Anal. Chem. **2009**, *81*, 2785–2790

Electrochemical Detection of Epidermal Growth Factor Receptors on a Single Living Cell Surface by Scanning Electrochemical Microscopy

Yasufumi Takahashi,[†] Takeshi Miyamoto,[†] Hitoshi Shiku,*[,†] Ryutaro Asano,[‡] Tomoyuki Yasukawa,[§] Izumi Kumagai,[‡] and Tomokazu Matsue*[,†]

Graduate School of Environmental Studies, Tohoku University, Aramaki Aoba 6-6-11-605, Sendai 980-8579, Japan, Graduate School of Engineering Studies, Tohoku University, Aramaki, Aoba 6-6-11-607, Sendai 980-8579, Japan, and Graduate School of Material Science, University of Hyogo, 3-2-1 Kouto, Kamigori-cho, Ako-gun, Hyogo 678-1297, Japan

A membrane protein on the surface of a single living mammalian cell was imaged by scanning electrochemical microscopy (SECM). The epidermal growth factor receptor (EGFR) is one of the key membrane proteins associated with cancer. It elicits a wide range of cell-type-specific responses, leading to cell proliferation, differentiation, apoptosis, and migration. To estimate EGFR expression levels by SECM, EGFR was labeled with alkaline phosphatase (ALP) via an antibody. The oxidation current of PAP (*p*-aminophenol) produced by the ALP-catalyzed reaction was monitored to estimate the density of cell surface EGFR. EGFR measurement by SECM has three advantages. First, a single adhesion cell can be measured without peeling it from the culture dish; second, it is possible to optimize labeling antibody concentrations by using living cells because detection of faradaic current is suitable for quantitative estimation in situ; and third, SECM measurements afford information on the expression state at the cell membrane at the single-cell level. In this study, we optimized the concentration of labeling antibody for EGFR at the cell surface and confirmed distinct differences in EGFR expression levels among three types of cells. SECM measurements were compatible with the results of flow cytometry.

Most membrane proteins function via intermolecular interactions. The epidermal growth factor receptor (EGFR), one of the typical membrane proteins associated with cancer, elicits a wide range of cell-type-specific responses, leading to cell proliferation, differentiation, apoptosis, and migration.[1−3] Since EGFR can trigger irregular cellular proliferation, it has been considered an attractive target molecule for cancer therapy.[4,5] Various methods have been introduced to study EGFR. These methods can be categorized into three main approaches. The first approach uses fluorescent measurement to clarify cellular signaling induced by EGFR. Dimerization of EGF−EGFR complexes and autophosphorylation of EGFR have been visualized by total internal reflection fluorescence microscopy.[6] In addition, fluorescence resonance energy transfer (FRET) imaging has been used to monitor the morphological changes induced by EGF stimulation.[7−9] In a microfluidic system where it is possible to induce local stimulation, laminar flows containing fluorescent-labeled EGF have revealed lateral propagation of EGFR signaling on single living cell surfaces.[10] The second approach examines EGFR as a target molecule for cancer therapy. The anti-EGFR antibody cetuximab, which is used for treatment of metastatic cancers of the colon, head, and neck, is known to prevent receptor activation, thus blocking downstream signaling.[4] The third approach involves the measurement of EGFR density and its distribution on cell surfaces. Radioisotope labeling,[11] fluorescent labeling,[12] and nanoparticle labeling[13,14] have been performed in order to estimate or image the expression level of EGFR. After stimulation of EGF, scanning near-field optical microscopy could reveal the EGFR distribution and estimate the EGFR cluster size.[15] Flow cytometry is one of the most useful systems for estimating the membrane protein expression level.[16] However, in flow cytometric measurements, cells need to be peeled off from the culture dish bottom; this process has the potential to cause unexpected changes in the state

* To whom correspondence should be addressed. Phone and fax: +81-22-795-7209. E-mail: shiku@bioinfo.che.tohoku.ac.jp (H.S.); matsue@bioinfo.che.tohoku.ac.jp (T.M.).

[†] Graduate School of Environmental Studies, Tohoku University.

[‡] Graduate School of Engineering Studies, Tohoku University.

[§] University of Hyogo.

(1) Ullrich, A.; Schlessingert, J. *Cell* **1990**, *61*, 203–212.
(2) Jaiswal, J. K.; Simon, S. M. *Nat. Chem. Biol.* **2007**, *3*, 92–98.
(3) Ishii, Y.; Yanagida, T. *Single Mol.* **2000**, *1*, 5–16.
(4) Ciardiello, F.; Tortora, G. *Clin. Cancer Res.* **2001**, *7*, 2958–2970.
(5) Asano, R.; Sone, Y.; Ikoma, K.; Hayashi, H.; Nakanishi, T.; Umetsu, M.; Katayose, Y.; Unno, M.; Kudo, T.; Kumagai, I. *Protein Eng.* **2008**, *21*, 597–603.
(6) Sako, Y.; Minoguchi, S.; Yanagida, T. *Nat. Cell Biol.* **2000**, *2*, 168–172.
(7) Clayton, A. H. A.; Tavarnesi, M. L.; Johns, T. G. *Biochemistry* **2007**, *46*, 4589–4597.
(8) Gadella, T. W. J.; Jovin, T. M., Jr. *J. Cell Biol.* **1995**, *129*, 1543–1558.
(9) Sorkin, A.; McClure, M.; Huang, F.; Carter, R. *Curr. Biol.* **2000**, *10*, 1395–1398.
(10) Sawano, A.; Takayama, S.; Matsuda, M.; Miyawaki, A. *Dev. Cell* **2002**, *3*, 245–257.
(11) Wrann, M. M.; Fox, C. F. *Bio. Chem.* **1979**, *254*, 8083–8086.
(12) Liu, W.; Howarth, M.; Greytak, A. B.; Zheng, Y.; Nocera, D. G.; Ting, A. Y.; Bawendi, M. G. *J. Am. Chem. Soc.* **2008**, *130*, 1274–1284.
(13) El-Sayed, I. H.; Huang, X.; El-Sayed, M. A. *Nano Lett.* **2005**, *5*, 829–834.
(14) Huang, X.; El-Sayed, I. H.; Qian, W.; El-Sayed, M. A. *J. Am. Chem. Soc.* **2006**, *128*, 2115–2120.
(15) Nagy, P.; Jenei, A.; Kirsch, A. K.; Szöllösi, J.; Damjanovich, S.; Jovin, T. M. *J. Cell Sci.* **1999**, *112*, 1733–1741.
(16) Kimmig, R.; Pfeiffer, D.; Landsmann, H.; Hepp, H. *Int. J. Cancer* **1997**, *74*, 365–373.

10.1021/ac900195m CCC: $40.75 © 2009 American Chemical Society
Published on Web 03/05/2009

of the cell surface. Fluorescent microscopy allows adhesion cell measurement, but it is not suitable for quantitative analysis because of photobleaching and autofluorescence of the cell itself.

Scanning electrochemical microscopy (SECM) has been successfully used to investigate various biological systems. This is because a localized chemical reaction under physiological conditions can be quantitatively characterized in situ in a noninvasive manner.[17-22] While in most analytical tools, the sample must be physically attached to the sensor, a feature of the SECM is the ability to set the detector, namely, the microelectrode, near the sample surface. Therefore, living cell measurement can be carried out in situ by SECM. We have previously developed SECM-based enzyme-linked immunosorbent assays (ELISA) for detecting antigen[23-27] and cytokine[28] molecules by using the sandwich methodology. Wittstock et al. reported on the characterization of antibodies immobilized on magnetic beads in order to improve the sample preparation of beads and sensitivity of ELISA.[29,30]

With the use of enzyme-labeled antibodies, it is possible to visualize receptor proteins on the living cell membrane for SECM measurement. Membrane protein measurement by SECM has three advantages. First, a single adherent cell can be measured without peeling it from the culture dish; second, optimization of the labeling antibody concentration is possible because faradaic current is suitable for quantitative estimation; and third, a faradaic current image corresponding to the expression state of the measured membrane protein is available at the single-cell level. However, there have been no reports in the literature on the application of SECM to membrane protein measurement. The current study is the first to use SECM to measure membrane protein.

EXPERIMENTAL SECTION

Chemicals. The primary antibodies (mouse anti-EGFR IgG [sc-120, Santa Cruz Biotechnology, Santa Cruz, CA], mouse anti-EGFR IgG FITC conjugated [sc-120 FITC, Santa Cruz Biotechnology, Santa Cruz, CA]), the secondary antibodies (alkaline phosphatase [ALP]-goat antimouse IgG [62-6522, Zymed], β-galactosidase[β-Gal]-goat antimouse IgG [A-106GN, American Qualex]), Diaphorase-1 (Dp, *Bacillus stearothermophilus*; Unitika Ltd.), NADH (Calzyme Laboratories, Inc.), a Biotin Labeling kit-NH_2 (Dojindo Laboratory), *p*-aminophenylphosphate monosodium salt (PAPP; LKT Laboratory Inc.), *p*-aminophenol (PAP; Wako Pure Chemical Industries), *p*-aminophenyl-β-D-galactopyranoside (PAPG; Wako Pure Chemical Industries), ferrocenemethanol ($FcCH_2OH$; Aldrich), and poly(dimethylsiloxane) (PDMS; Dow Corning Toray Co., Ltd.) were purchased and used as received. All other chemicals were used as received. All the solutions were prepared using distilled water obtained from a Milli-Q (Millipore, Japan).

Cell Culture. A normal Chinese hamster ovary (CHO) and cells derived from human epidermoid carcinoma cell line A431 were donated from the Cell Resource Center for Biomedical Research (Tohoku University). The EGFR/CHO (CHO transfected with EGFR) used in this study were prepared according to the literature.[5]

Normal CHO and A431 cells were cultured in an RPMI-1640 medium (Gibco Invitrogen, Tokyo, Japan) containing 10% fetal bovine serum (FBS; Gibco), 50 μg/mL penicillin (Gibco), and 50 μg/mL streptomycin (Gibco) at 37 °C in a humidified atmosphere containing 5% CO_2. The EGFR/CHO cells were cultured in RPMI-1640 medium (Sigma) containing 10% fetal bovine serum (FBS, Gibco), 50 μg/mL G418 (Nacalai Tesque) at 37 °C in a humidified atmosphere containing 5% CO_2.

Labeling EGFR with Enzymes via Antibodies. EGFR was labeled with ALP, β-Gal, or Dp via antibodies for electrochemical detection. For ALP labeling, the cells were incubated for 90 min in RPMI-1640 with anti-EGFR antibody (1 μg/mL), followed by thorough washing with RPMI-1640. Cells were then incubated for 90 min in RPMI-1640 with ALP-labeled secondary antibody (1 μg/mL). EGFR was also labeled with β-Gal using the same procedure as that used for ALP labeling.

For labeling with Dp, the cells were incubated for 60 min in RPMI-1640 with a biotin-labeled anti-EGFR antibody (1 μg/mL, 100 μL). After thorough washing with phosphate buffered saline (PBS), the cells were incubated for 30 min in RPMI-1640 containing bovine serum albumin (BSA, 10 mg/mL) to block physical adsorption of interfering proteins. The cells were then incubated for 30 min in RPMI-1640 with avidin (10 mg/mL). After extensive washing with PBS, the cells were treated in RPMI-1640 with biotin-labeled Dp (25 μg/mL) for 40 min. Biotinylation of anti-EGFR antibody and Dp was carried out using a Biotin Labeling kit-NH_2.

SECM Measurements. We used two EGFR-detection methods for SECM measurements, the substrate generation/tip collection mode and the feedback mode (Figure 1). The measurements were conducted using a HEPES-based saline solution (10 mM HEPES, 150 mM NaCl, 4.2 mM KCl, and 11.2 mM glucose; pH 9.5) containing 4.7 mM PAPP and 10% FBS for detection of ALP-labeled EGFR. HEPES-based saline solution (pH 7.5) containing 7.4 mM PAPG was used for the detection of β-Gal-labeled EGFR, and HEPES-based saline solution (pH 7.5) containing 0.5 mM $FcCH_2OH$ was used for Dp-labeled EGFR.

The potential of the microelectrode probe was set at +0.30 V vs Ag/AgCl for the detection of ALP- and β-Gal-labeled EGFR. ALP and β-Gal catalyzed the hydrolysis of PAPP and PAPG, respectively. Both enzyme reactions yielded PAP as an enzymatic

(17) Shiku, H.; Shiraishi, T.; Ohya, H.; Matsue, T.; Abe, H.; Hoshi, H.; Kobayashi, M. *Anal. Chem.* **2001**, *73*, 3751–3758.
(18) Torisawa, Y.; Ohara, N.; Nagamine, K.; Kasai, S.; Yasukawa, T.; Shiku, H.; Matsue, T. *Anal. Chem.* **2006**, *78*, 7625–7631.
(19) Bard, A. J.; Li, X.; Zhan, W. *Biosens. Bioelectron.* **2006**, *22*, 461–472.
(20) Amemiya, S.; Guo, J.; Xiong, H.; Gross, D. A. *Anal. Bioanal. Chem.* **2006**, *386*, 458–471.
(21) Schulte, A.; Schuhmann, W. *Angew. Chem., Int. Ed.* **2007**, *46*, 2–20.
(22) Wittstock, G.; Burchardt, M.; Pust, S. E.; Shen, Y.; Zhao, C. *Angew. Chem., Int. Ed.* **2007**, *46*, 1584–1617.
(23) Shiku, H.; Matsue, T.; Uchida, I. *Anal. Chem.* **1996**, *68*, 1276–1278.
(24) Wittstock, G.; Yu, K.; Halsall, H. B.; Ridgway, T. H.; Heineman, W. R. *Anal. Chem.* **1995**, *67*, 3578–3582.
(25) Shiku, H.; Hara, Y.; Matsue, T.; Uchida, I.; Yamauchi, T. *J. Electroanal. Chem.* **1997**, *438*, 187–190.
(26) Kasai, S.; Yokota, A.; Zhou, H.; Nishizawa, M.; Niwa, K.; Onouchi, T.; Matsue, T. *Anal. Chem.* **2000**, *72*, 5761–5765.
(27) Yasukawa, T.; Hirano, Y.; Motochi, N.; Shiku, H.; Matsue, T. *Biosens. Bioelectron.* **2007**, *22*, 3099–3104.
(28) Kasai, S.; Shiku, H.; Torisawa, Y.; Nagamine, K.; Yasukawa, T.; Watanabe, T.; Matsue, T. *Anal. Chim. Acta* **2006**, *566*, 55–59.
(29) Wijayawardhana, C. A.; Wittstock, G.; Halsall, H. B.; Heineman, W. R. *Anal. Chem.* **2000**, *72*, 333–338.
(30) Wijayawardhana, C. A.; Wittstock, G.; Halsall, H. B.; Heineman, W. R. *Electroanalysis* **2000**, *12*, 640–644.